Universidade do Minho
Escola de Engenharia

Vânio Miguel Rodrigues Ferreira

Mapping local thickness from CAD models to finite element meshes

Outubro de 2010

Universidade do Minho
Escola de Engenharia

Vânio Miguel Rodrigues Ferreira

Mapping local thickness from CAD models to finite element meshes

Master in Informatics

supervision of:
Doctor Luís Paulo Peixoto dos Santos
and
Doctor Ricardo João Ferreira Simões

Outubro de 2010

Acknowledgments

I would like to thank the FORD Motor Company for supporting my Master's degree studies.

Thank you to my supervisors Dr Luís Paulo Peixoto Dos Santos and Dr Ricardo João Ferreira Simões for their advice during this project. Their comments and guidance throughout this research have helped me to challenge my ideas and justify my reasoning. Thank you also to Markus Franzen and Omar O. Ghouati, from FORD Motor Company, for providing feedback from an industrial viewpoint.

Most of all I want to thank my family for their love and support, and my girlfriend Sara Teixeira for her endless support and patience.

Abstract

The manufacturing industry submits digital models of parts to numerical simulations in order to determine their structural behavior under different conditions. The accuracy of such simulations, often based on finite element methods, depends on the amount and diversity of information available about these parts. Some of this information might not be directly available from the digital models, but might, in some cases, be estimated by post-processing these models.

A concrete example is information about the local thickness of automotive parts, which might, if available, significantly increase the accuracy of finite element crash simulations. Such simulations are fundamental to allow the automotive industry to predict thermoplastic parts deformation and the obtained results are obviously dependent on the accuracy of the provided input data. One of the main methods currently employed for car crash simulations is finite element analysis and the most commonly used finite element meshes are mid-plane meshes (which are two-dimensional but can have a thickness assigned to each element). However, the problem is that three dimensional models of the parts do not include information about part thickness. For years, the industry has typically resorted to using averaged thickness throughout the part instead of a precise per mid-plane mesh element thickness, since that information is not readily available from current models/methods. However, having a precise thickness mapping in the mid-plane mesh would significantly improve the overall simulation accuracy, and thus, its usefulness. Since thickness is almost always not uniform along the part, having to assume an average thickness throughout the entire mid-plane mesh is a very rough approximation and induces unnecessary error in the calculations.

This study proposes and compares two approaches based on ray tracing and nearest neighbor 3D range searches for extracting thickness information from the three dimensional models and make it available on the mid-plane finite element meshes used for numerical simulations. This will be achieved by processing the part geometry and measuring its thickness along the appropriate direction. A systematic quantitative analysis of the accuracy of both approaches is presented, as well as a thorough identification of particular geometric arrangements under which their accuracy can be compromised. These results enable the identification of each approaches's weaknesses leading towards a integrated approach to the problem that combines the estimates produced by each approach: using both approaches' estimates to assign them a confidence given their relative variations within some neighborhood. Finally a method is presented that allows to detect inaccuracies in the thickness estimated by the approaches, providing an automatic way of improving their accuracy. A sensitivity study is also presented, in order to assess the method's efficiency.

Resumo

A indústria de manufactura recorre a modelos digitais de peças de forma a determinar, a partir de simulações numéricas, o seu comportamento estrutural quando sujeitas a várias condições. A precisão destas simulações, muitas vezes baseadas em métodos de elementos finitos, depende da quantidade e diversidade de informação disponível. Parte desta informação pode não estar directamente disponível a partir dos modelos digitais, mas pode, em alguns casos, ser estimada através do seu pós-processamento.

Um exemplo concreto é a informação sobre a espessura local de peças de automóveis, que pode, se disponível, aumentar significativamente a precisão das simulações de acidentes baseadas em métodos de elementos finitos. Estas simulações são fundamentais para permitir à indústria automóvel prever a deformação de peças termoplásticas, e os resultados obtidos são, obviamente, dependentes da precisão dos dados fornecidos. Um dos principais métodos actualmente empregues nestas simulações é a análise de elementos finitos, cujas malhas mais usadas são as "mid-plane" (que são bidimensionais mas podem ter uma espessura associada a cada elemento). O problema é que a informação sobre a espessura não está directamente acessível a partir dos modelos tridimensionais das peças. Durante anos, a indústria assumiu, tipicamente, uma espessura média ao longo de toda a peça em vez da espessura exacta de cada elemento da "mid-plane", uma vez que esta não se obtém prontamente a partir dos modelos/métodos. Contudo, um mapeamento exacto da espessura da "mid-plane" poderia melhorar significativamente a precisão, e desta forma, a sua utilidade. Uma vez que a espessura não é sempre uniforme, ter que assumir uma espessura média ao longo de toda a "mid-plane" é uma aproximação muito grosseira e induz, desnecessariamente, erros nos cálculos.

Este estudo propõe e compara duas abordagens baseadas em "ray-tracing" e "nearest neighbor 3D range searches" para extrair informação sobre a espessura de modelos tridimensionais e disponibilizá-la nas malhas de elementos finitos "mid-plane" usadas para simulações numéricas. Esta informação é extraída através do processamento da geometria da peça e da medição da espessura ao longo da direcção apropriada. Uma análise sistemática e quantitativa da precisão de ambas as abordagens é apresentada, bem como de uma identificação completa das disposições geométricas nas quais a precisão das abordagens é comprometida. Estes resultados permitem a identificação das falhas de cada abordagem, sugerindo uma abordagem integrada que combina as estimativas produzidas por cada abordagem: usando ambas as estimativas de cada abordagem para lhes atribuir uma confiança dado as variações relativas dentro de uma vizinhança. Finalmente é apresentado um método que permite detectar imprecisões na espessura estimada pelas abordagens, fornecendo uma forma automática de melhorar a precisão. Uma análise de sensibilidade é também apresentada, de forma a verificar a eficácia do método.

Contents

List of Figures

List of Tables

Chapter 1

Introduction

1.1 Context

Modern product design and development processes are characterized by the extensive use of computer modeling and computer simulation tools and techniques. Numerical simulation of real-world problems has become standard practice among manufacturers worldwide, helping to reduce costs and meet short time-to-market windows. At the same time, simulation has helped improve product quality, optimize materials usage, and address increasingly stringent governmental safety and environmental regulations. In the case of the automotive industry, the concern of passenger safety and the demanding of highly fuel-efficient and environmental friendly vehicles lead the automotive companies to use alternative design techniques and manufacturing materials, such as the injection model and parts made of plastic, respectively. The parts made of plastic materials have become pervasive in many of today's engineering applications, including those with very demanding specifications, such as the automotive industry. However the properties of these parts are particularly difficult to predict due to the intrinsic complex behavior of those materials. It is then vital to find adequate methods for modeling and simulating the parts' physical properties, manufacturing analysis and service conditions, so they maintain or improve the vehicle performance compared with that achieved by the conventional materials.

These analyses are executed through the use of Computer-Aided Engineering (CAE) software, using geometry information from Computer-Aided Design (CAD) models of parts, and usually a dimensionally abstracted model is used over the full detailed model, so that the analysis has less computational costs [Arm94, LG05]. In this case, the detailed model needs to be simplified to a mid-plane mesh, which should retain all the important topology information. However, within the area of crash simulation of thermoplastic parts, the accuracy of the simulation process is highly dependent on the amount and diversity of information available about these parts, particularly about

the local thickness, which plays a significant role for accurate deformation and fracture behavior prediction. Due to the fact that most thermoplastic parts in the interior of vehicles are injection molded, the actual thicknesses vary significantly throughout thermoplastic parts. Currently there is no automated and precise way to use the exact thickness distribution information existent in CAD files (like IGES) within two dimensional crash meshes, which are mainly used in full car crash simulations.

1.2 Finite Element Analysis

One of the main methods currently employed for car crash simulation of thermoplastic parts is Finite Element Analysis (FEA). FEA is a numerical approach for calculating approximate solutions of partial differential equations and integral equations, enabling the numerical solution of many complex problems in structural mechanics, and is the standard approach for complex systems, particularly in the industry setting [Yan86]. The entire geometric domain of the part/system under study is discretized and modeled by a mesh (whether a mid-plane two-dimensional mesh, or a full three-dimensional surface or solid mesh), comprised of a large set of finite elements (which can be of several simple geometries) that intersect at points termed nodes [FG00, Ede01, TWM85, SPW08, KPSC06]. Elements are then assigned properties, which can be physical (e.g. thickness, density, Young's modulus, tensile strength), thermal, electric, or others. This method was initially proposed in the 1950s for airframe and structural analysis [WG66]. In 1973, Strang and Fix [SF73] provided a rigorous mathematical foundation, and enabled its expansion to many new applications. Aside from its major application to structural mechanics, FEA has been used in a large variety of fields, including acoustics [BNPvE08], fluid dynamics [Löh08], medicine [HO08], and many others.

1.3 Motivation

Since there is no automated way to include the information about part exact thickness, an average or design thickness is assumed throughout the entire mid-plane mesh. As thickness is not always uniform along the part, this is a very rough approximation and induces unnecessary errors in the calculations. In order to improve the accuracy of the simulations, this thesis aims to extract thickness from the three dimensional models and make these available on the mid-plane finite element meshes used for numerical simulations. It proposes and compares two techniques to estimate local thicknesses from geometric models of cars' thermoplastic parts based on ray tracing and nearest

neighbor 3D range searches allowing tagging each mesh element with its associated local thickness, thus empowering accurate car crash simulations. The approaches' behavior and accuracy is subjected to a thorough study, allowing the identification of each approaches' weaknesses, sugesting an integrated approach that combines the estimates produced by each approach.

1.4 Framework

The work performed under this thesis was framed by project CAD2FE, developed in cooperation between the University of Minho and Ford Motor Company. The primary contribution was a methodology to evaluate local thicknesses from CAD models of industrial parts from Ford, materialized in a tool, named CAD2FE, that will be used in a daily-basis way at Ford, helping engineers evaluate the performance of injection molded parts under service condition with more accuracy, enabling faster design cycles and ultimately more safer cars.

1.5 Outline

Chapter 2 provides a review of the relevant applications of the FEM and of the two thickness estimation approaches in several areas of engineering and science. Chapter 3 describes the two thickness estimation approaches that were developed, and the some of their limitations. Chapter 4 presents an systematic quantitative analysis of the accuracy of both thickness estimation approaches. Chapter 5 describes a method for improving the thickness accuracy that has been developed, its methodology and a sensitivity analysis. In Chapter 6 conclusions are drawn and chapter 7 discusses future work.

Chapter 2

Literature Review

2.1 Finite element methods

In order to study and analyze many real world phenomena, like mechanical systems, one must write the governing equations and boundary conditions for the problem in hand. This can be addressed by deriving differential equations or equivalent statements, which imply an infinite number of elements. These systems, usually termed *continuous*, can only then be solved exactly by mathematical manipulation. Solving these systems by hand are often impossible, due to their complexity and dimensions. Also, as their are *continuous*, they cannot be solved in digital computers, whose capacity is finite. Therefore it is necessary to obtain approximate numerical solutions rather than exact closed-form solutions. The Finite Element Method (FEM) is the dominant technique for discretization and analyzing complex problems in the engineering areas of automotive, aerospace and civil [HDSB01]. Other numerical analysis methods have evolved over the years, such as finite difference [ATP84]. However, they are not so well suited for irregular grid geometries or unusual specification of boundary conditions as FEM.

FEM is the leading technique for analyzing the behavior of solid and structural problems. It can be applied to analyze applications of contact mechanics, which are of great importance in industry related to mechanics, civil engineering, environment and medical applications [Wri06]. The range of such applications covers problems like foundations, the connections of structural members by bolts or screws, the rolling contact of tires and the impact of cars against building structures, which are some of the most challenging and complex contact problems. Car crash simulations are of great interest to the automotive industry since using numerical simulation can reduce development and costs of modern cars [Wri06]. Such simulations have complex geometries or experience large deformations, so the majority of the industry uses numerical methods to solve them, among which FEM is one of the most used. Another important field is Fluid Mechanics, which is concerned with

the motion and interaction of gases and liquids [HDSB01]. The equations of motion are known as Navier-Stokes equations, and are the basis for solving most of fluid mechanics problems. FEM can be applied to fluids by adapting its formulation with the Navier-Stokes equations [HDSB01]. The use of FEM instead of the classical finite volume method gives the benefit of generally better stability/robustness of the solution, although care must be taken to ensure a conservative solution. An example of successfully applying FEM to solve fluid mechanical problems is shown on [BA08], where aerodynamic and aeroelastic analyses previously performed in a wind tunnel are simulated with FEM. Drop test simulation involves physical dropping devices to test their quality and reliability. However due to the size of some devices, particularly electronic ones, it is difficult to collect information about the drop phenomenon, especially the inside response. In [WLL+05] the numerical simulation of drop testing is solved by FEM, which is the only numerical method available to solve such simulation. The results obtained were good and the author suggests that the physical drop test can be replaced by the virtual-simulation.

As applied to solid and structural problems, the finite element method is the leading technique for analyzing the behavior of structures when subjected to a variety of loads. The loads may be static or dynamic, and the structural responses can be linear or non-linear, with varying degrees of complexity. The underlying theory of the method is now well established, with many books and courses providing adequate explanations of the theory [ZT00, HDSB01].

2.2 Ray tracing

In computer graphics ray tracing can be described as a technique that *"simulates global interaction by explicitly tracking infinitely thin beams, or rays, of light as they travel through a scene from object to object"* [?]. Basically, ray tracing simulates the path that a ray travels from an origin to infinity or until it intersects some object, possibly creating reflections by "shooting" more rays from the point intersected. It is usually used in computer graphics as a global reflection model and it performs best when dealing with specular interaction, producing high-quality photo-realistic images when the scene consists of shiny, mutually reflective objects.

Although ray tracing is a popular technique in computer graphics' field, its applications can be seen in other fields of science and engineering. By simulating waves of energy, ray tracing can play an important role in seismology, seismic exploration, and the interpretation of seismic measurements [Č01]. By assuming that there exist some distance where the ray is locally straight, the ray tracer will advance the ray over this distance. At this point the ray tracer can compute a new direction of the ray, based on the existence of objects, or other properties. This process is repeated until a complete path

is generated. [RHS08] provides a review of a variety of ray based solvers for locating ray paths. Changing the "ray" type to electromagnetic waves, ray tracing can be used to simulate the behavior of radio signals as they propagate through indoor or outdoor environments, such as the ionosphere. Depending on the environment an adequate representation of the propagation model is essential, since the ray may be transmitted and received by different mechanisms. Also, different environments have different obstacles, which need to be incorporated to the ray tracer. Examples of such applications can be found in [SR94, GBGP02] and [BT71, KGW+99] for inside and outside environments, respectively. In the fields of Computer Aided Engineering (CAE), ray tracing was also proved to be useful. In [KLP06] ray tracing is used to design reflectors of an automobile headlight. As the appearance of a modern car is strongly characterized by the aerodynamic and stylistic aspects of the headlamps, and each specific car model has a different body profile, ray tracing helps the design process by assessing if the headlamp model provides the requirement illumination pattern to illuminate the road surface. In [WBDS03] it is refereed the use of an interactive ray tracer to visualize the reflections of the car's dash board in the side window, where it might interfere with backward visibility through the outside mirror at night. Also as computer graphics can be fully utilized in almost all the stages of the product development cycle of automotive and aerospace industries [SK08] an interactive visualization of complex CAD models is essential. As ray tracing exhibit logarithmic time complexity with the use of acceleration structures (e.g. kd-tree) [WH06] ray tracing can be used to achieve such interactive visualization [DWS04]. Other applications include Ocean Acoustics, Optical Design, Plasma Physics and Virtual X-Ray imaging techniques.

2.3 Nearest neighbor problem

Finding nearest neighbors is among the most fundamental problems in computational geometry and in the study of searching algorithms in general [AMN+98]. It is not, therefore, surprising that nearest neighbor is used in so many engineering and scientific fields. Such algorithm can be used in motion planning, such as path planning algorithms and graph of collision-free paths [AL02]. It can also be used to study contact searching in FEM: computing the distances between elements of the same or different CAD datasets it is possible to assess for collisions [HC]. For the field of pattern classification [CH67] nearest neighbor is a problem with significant importance. Pattern classification can be described as "finding r functions, $g1, ..., gr$, such that a pattern x is in class i if $gi(x)$ is the optimal value among $g1(x), ..., gr(x)$ [Cha74]. Content-based image retrieval, which is important in multimedia databases, can use nearest neighbor as an algorithm for possible query similarities: representing images as d-dimensional feature vectors, and defining the similarity between the images by a distance function between their feature

vectors (e.g. Euclidean space) [FTAE02, BBKK97, BKK96], it is possible to find images most similar to a given image. Searching for "similar shapes" can also be achieved with nearest neighbor, which can have broad applications in electronic commerce, photo-journalism, and medical use [KSF+96]. Another area where nearest neighbor searching is very important is in data compression [GG91]. Data compression is achieved, similarly to pattern classification, by vector quantization. Vector quantization consists in grouping sets of points that have approximately the same number of neighbors. Each group can be represented by its centroid point, which can consist in a vector that uniquely defines the characteristic of that group.

2.4 Conclusion

With the advent of FEM and the development of finite element pre and post processors, scientist and engineers could simulate many unthinkable problems. The discretization allowed by FEM provides a way to reduce the complexity of the problem domain, and hence the process of sub-dividing all systems into their individual components or 'elements', whose behavior is readily understood, and then rebuilding the original system from such components to study its behavior. Ray tracing and nearest neighbor also proved to be valuable techniques to address several problems in different field of science and engineering.

Chapter 3

Thickness estimation

3.1 Computer-aided models and mid-plane meshes

In order to analyze the physical properties and services conditions of thermoplastic parts, Computer-Aided Design (CAD) models are created that represent the part's surface. These CAD models (from now on, just models) can represent the part's surface with Non-uniform rational B-spline (NURBS) geometry and/or boundary representation (B-rep) data (expressed by the concept of geometric continuity) or by a polygon mesh (discretization). The analysis performed to the models are executed within Computer-Aided Engineering (CAE) software (which can be integrated with a CAD package or a separate application), and usually a dimensionally abstracted model is used over the full solid, so that the analysis has less computational costs [Arm94, PCC09]. This abstracted model, termed mid-plane mesh, is generated by a process of discretization [1] of the geometry of the thermoplastic part and results in a mesh that ideally runs inside its closed surface and parallel to it. Figures 3.1, 3.2 and 3.3 show examples of the resulting mid-plane meshes obtained for a two dimensional model and for a simple and complex three dimensional models, respectively. However, during the generation of mid-plane meshes the information about the part's local thickness is not mapped to the mid-plane mesh, which is crucial to allow accurate behavior prediction in car crash simulations. Also, the currently used approach to generate mid-plane meshes is based on highly time-consuming manual work resulting in CAE meshes with limited accuracy (dark green regions in figure 3.3), which prevents fully exploring the advantages of modeling and simulation tools.

Intuitively, in such cases as depicted in figures 3.1 and 3.2 the thickness at the centroid[2] of each mid-plane mesh element is the sum of the distances be-

[1] In mathematics, discretization concerns the process of transferring continuous models and equations into discrete counterparts - Wikipedia

[2] The center of mass of a two-dimensional planar lamina or a three-dimensional solid - Wolfram mathworld.

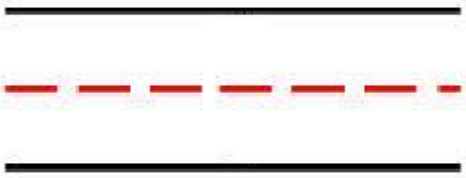

Figure 3.1: Solid black lines represent the part's geometry, the red dashed line represents the midplane mesh.

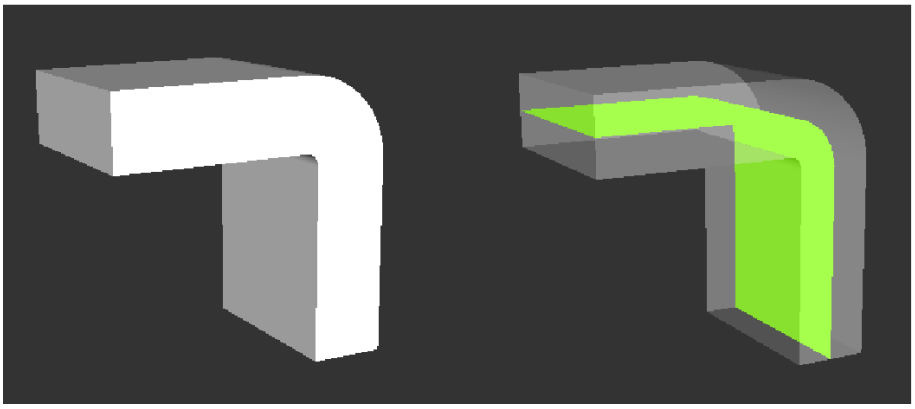

Figure 3.2: A simple CAD model (left) and its midplane mesh representation (green surface inside the translucid model, right).

tween this centroid and some surface point on each side of the element. With this definition in mind two thickness estimation approaches are proposed.

3.2 Thickness estimation approaches

3.2.1 Ray tracing

Ray tracing [App68, Whi80] consists on determining the closest geometric primitive to a point p along a certain direction by shooting a ray with origin in p and through that direction. The geometric primitive intersected by the ray and closest to p is the closest primitive. This algorithm is used in several applications, the most common being the rendering of images.

This algorithm can be adapted to the process of local thickness estimation. A ray is shot for each side of the mid-plane mesh element, with origin on the element's centroid and direction equal to the element's normal. Ideally, each of these rays intersects the part's geometry; the sum of both intersections' distances is taken as an estimate of the part's local thickness (see figure 3.4).

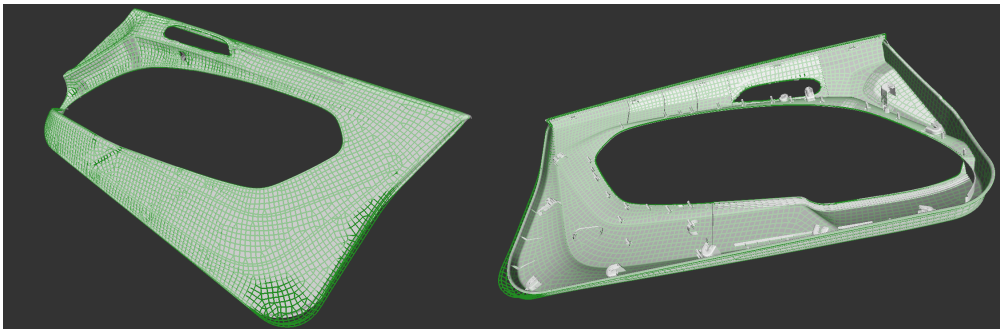

Figure 3.3: Different views of a car door model (grey) and its mid-plane mesh representation (green). Ideally the mid-plane mesh runs inside the model's surface, but in reality it might extend outside (dark green regions).

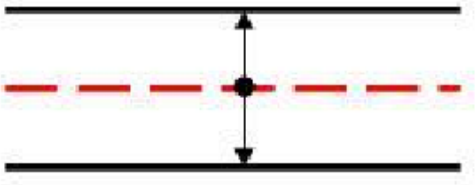

Figure 3.4: Rays shoot from each side of mid-plane mesh, with origin and direction equal to the element's centroid and normal.

Intersection algorithm

To test for ray/triangle intersection, an algorithm based on barycentric coordinates [Yiu00] was implemented. Barycentric coordinates provide a way to parameterize a triangle (with vertices's $p0$, $p1$ and $p2$) in terms of two variables, $\beta 1$ and $\beta 2$:

$$p(\beta 1, \beta 2) = (1 - \beta 1 - \beta 2)p0 + \beta 1 p1 + \beta 2 p2 \text{ (A1)}$$

The conditions on $\beta 1$ and $\beta 2$ are:

$$\beta 1 \geq 0, \beta 2 \geq 0 \text{ and } \beta 1 + \beta 2 \leq 1$$

Barycentric coordinates also allow to interpolate across the surface of the triangle, providing a way to assess if a point p is inside the triangle.
To derive an algorithm to intersect a ray with a triangle, the ray needs to be defined in terms of its origin and a direction vector, which defines a ray as set of points on:

$$\text{R(t)} = \text{Rorigin} + \text{Rdirection} * \text{t, where t} > 0 \text{ (A2)}$$

The direction vector needs to be normalized, otherwise t will represent the distance in terms of the length of the direction vector. Substituting A1 into the triangle equation A2:

$$\text{Rorigin} + \text{Rdistance} * \text{t} = (1 - \beta 1 - \beta 2)p0 + \beta 1 p1 + \beta 2 p2$$

Solving this equation will give us both the barycentric coordinates of the intersection point as well as the distance along the ray. Note that, if the barycentric coordinates are less than zero or greater than one, then the point is outside the triangle, so no intersection occur.

3.2.2 Nearest neighbor

Nearest neighbor consists in computing/searching for the neighborhood about a point, usually in a two or three dimensional Euclidean space [Yia93]. Given a set S of points, in a metric space [3] M and query point $q \in M$, nearest neighbor finds the closest point in S to q.

Figure 3.5 illustrates a set of points in a two dimensional Euclidean space, including a query point q whose nearest point is sought (left) . By computing the euclidean distance between query point q and all the points in the set, the nearest neighbor algorithm finds the nearer point in the set to q (right).

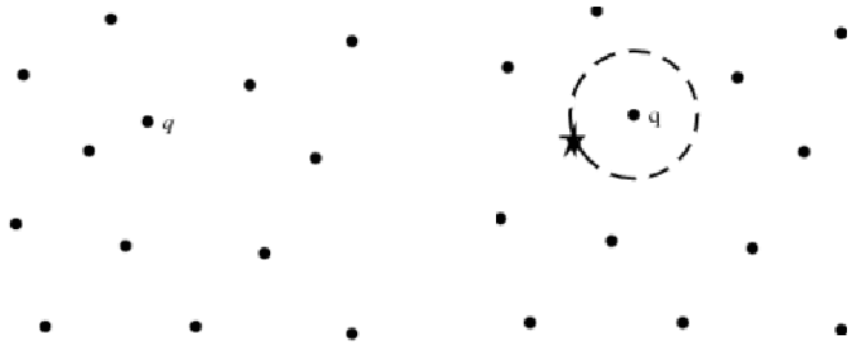

Figure 3.5: Left image shows a set of elements distributed in a two dimensional Euclidean space and a query point q whose nearest point is sought. The right image shows the nearer point to the query point q, computed with the nearest neighbor algorithm.

This algorithm can be adapted to the process of local thickness estimation. A search on the model's surface geometry is performed to locate which point is nearer to the mid-plane mesh element centroid [dB08]. Figure 3.6 illustrates this process; the dashed circle represents the search domain, which grows until the search algorithm returns a valid point on the model's surface. Actually, two such searches are performed to locate two points, each on a different

[3] http://mathworld.wolfram.com/MetricSpace.html

side of the mid plane mesh element. The sum of the distances from the element's centroid and these two points is taken as an estimate of the part's local thickness.

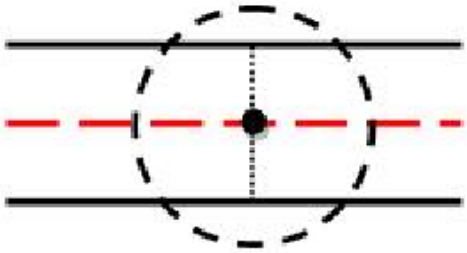

Figure 3.6: The dashed circle represents the nearest neighbor search domain.

Algorithm

To compute the minimum distance between a point p (the centroid of the mid-plane mesh element) and a triangle T (the elements of the surface) parameterized with barycentric coordinates

$$\mathrm{T}(\beta 1, \beta 2) = \beta + \beta 1 p1 + \beta 2 p2$$

where

$$(\beta 1, \beta 2) \in D = \{(\beta 1, \beta 2) : \beta 1 \in [0,1], \beta 2 \in [0,1], \beta 1 + \beta 2 \leq 1\}$$

it is necessary to locate the values $(\beta 1', \beta 2') \in D$, corresponding to the point r on the triangle T closest to p. This can be achieved by finding the minimum of the squared-distance function, defined as:

$$\mathrm{Q}(\beta 1, \beta 2) = |\mathrm{T}(\beta 1, \beta 2) - p^2|$$

Since Q is a continuous function, by the extreme value theorem [4], a minimum must exist. Computing the gradient $\nabla \mathrm{Q}$ so that $\nabla \mathrm{Q}(\beta 1', \beta 2') = (0,0)$ the global minimum can be found either in the interior of T, if $(\beta 1', \beta 2') \in D$, or on the boundary of T, otherwise. In [Ebe] a detailed explanation is provided of how to test for the boundaries of D and how to compute the distance in these cases.

After computing the closest point r of T to p is necessary to assess if T is a valid neighbor. If the dot product between the normal of the mid-plane mesh element and the vector that goes from p to r is positive then T is a valid neighbor, else T is discarted.

[4] http://mathworld.wolfram.com/ExtremeValueTheorem.html - Wolfram MathWorld

3.3 CAD2FE tool

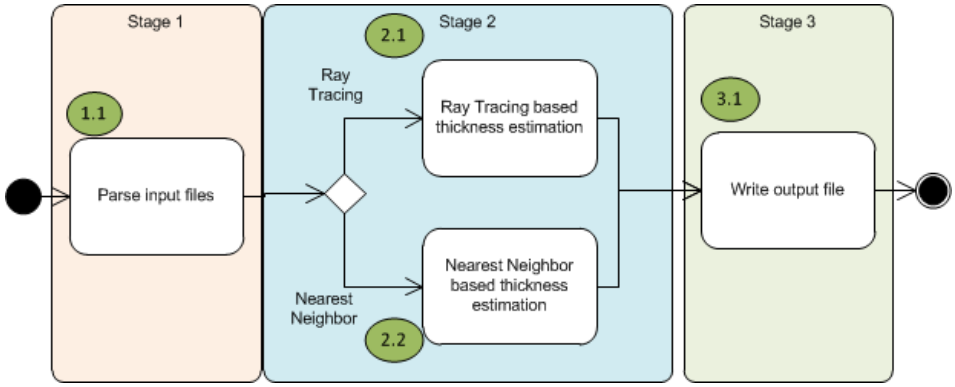

Figure 3.7: UML activity diagram. The diagram illustrates the behavior and overall data flow of the CAD2FE tool.

Figure 3.7 shows an Unified Model Diagram (UML) that illustrates the behavior and overall data flow of the CAD2FE tool. The activities presented in the diagram can be reduce to three main stages (a set of processes or activities in UML nomenclature): parsing the geometric information from the input files (the surface from VRML files and the mid-plane mesh from RADIOSS V44/9.0 and LS-DYNA); estimating the thickness of mid-plane elements with one of the proposed approaches; and writing the thickness results to an output file.

3.4 Approaches behavior

In the ideal case, as depicted in figure 3.4 and 3.6, both approaches return exactly the same thickness estimate. Real parts, however, may include complex geometric configurations. For example, the part's geometry may change in unpredictable ways (figure 3.9) and/or include ribs (figure 3.10) or other features[5]. It is then important to test how both approaches behave in these situations (and with behave we mean estimate the best possible local thicknesses of a model) .

Virtual test specimens

Figures 3.8, 3.9 and 3.10 show three virtual test specimens (termed A1, A2 and A3, respectively) that represent different, but common, simple geometric configurations of real world parts. Specimen A1 and A2 represent a "smooth"

[5] *Features are generic shapes or characteristics of a product with which engineers associate certain attributes and knowledge useful to reasoning about that product. Features encapsulate the engineering significance of portions of the product geometry.* [J.J95]

and a "sudden" change in the shape of the part's surface, respectively, and specimen A3 represent a rib in the part's surface. For specimen A1, figure 3.11 shows that both approaches behave correctly. The rays shoot by ray tracing approach intersect the correct elements in the surface, while the nearest neighbor approach computes the correct nearer elements of the surface. For specimen A2, figure 3.12 shows that only the nearest neighbor approach behaves correctly. The rays shoot by the ray tracing approach from the oblique elements in the mid-plane mesh do not intersect the correct oblique elements of the part's surface. The estimated thickness by the ray tracing approach is thus much larger than expected. While the nearest neighbor approach seems to solve this issue, it fails to estimate the correct thickness of some mid-plane elements of specimen A3 (figure 3.13), "smoothing out" local thickness variations.

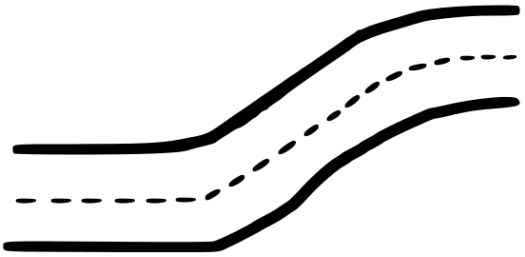

Figure 3.8: Virtual specimen A1. The specimen's surface has a "smooth" change in its shape. (Solid black lines represent the surface, dashed lines represent the mid-plane mesh).

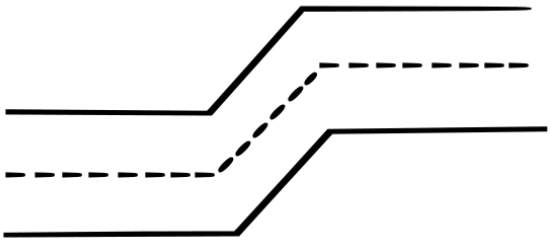

Figure 3.9: Virtual specimen A2. The specimen's surface has a "sudden" change in its shape. (Solid black lines represent the surface, dashed lines represent the mid-plane mesh).

The three virtual test specimens show that both approaches behave differently and that even in models with a simple geometric configuration, both approaches can estimate inaccurate values of thickness. However, real world parts can be far more complex than these simple specimens, so it is fundamental to test how both approaches behave with such complex geometries. Another important problem that may arise with the complexity of real world parts is that their mid-plane mesh representations may not be accurate/detailed. The mid-plane mesh may incorrectly approximate the complex

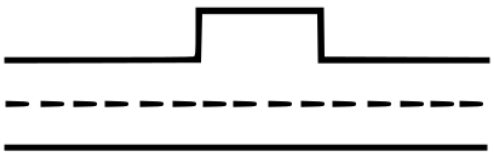

Figure 3.10: Virtual specimen A3. The specimen's surface includes a rib (Solid black lines represent the surface, dashed lines represent the mid-plane mesh).

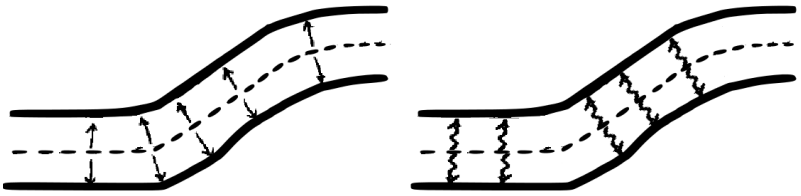

Figure 3.11: Both ray tracing and nearest neighbor approaches (left and right, respectively) behave correctly. (Solid black lines represent the surface, dashed lines represent the mid-plane mesh).

shapes of the model's surface, or even ignore some features, as they only introduce complexity to the generation of the mid-plane mesh and do not add any value to the finite element analysis [Arm94, PCC09].

B-Pillar Trim

To test how both approaches behave with real world parts, FORD provided two mid-plane meshes representing a model of a B-Pillar Trim. These mid-plane meshes were generated with different levels of granularity, corresponding to a coarse and fine representations of the model. Figure 3.14 shows the B-Pillar Trim model (top) and the the coarse (bottom left) and fine (bottom right) mid-plane meshes representations. The figure also reveals how the level of granularity can affect the accuracy and level of detail achieved by the mid-plane mesh representation of the model. Comparing both mid-plane meshes, it becomes easy to verify that the coarse mid-plane mesh is a poor representation of the model's geometry, as even some of the model's features were ignored during the generation of the mid-plane mesh. This is further demonstrated by figure 3.15 where the analogy between the coarse mid-plane mesh and the model's geometry becomes clear: in several regions of the model (the visible green regions), the mid-plane mesh runs outside the boundaries of the surface. The coarse mid-plane mesh is thus, an inaccurate representation. In contrast figure 3.16 shows how the fine mid-plane mesh is an accurate and detailed representation of the model.

Figures 3.17 and 3.18 show the thickness estimates (normalized to 1mm) obtained with the ray tracing approach for the coarse and fine mid-plane

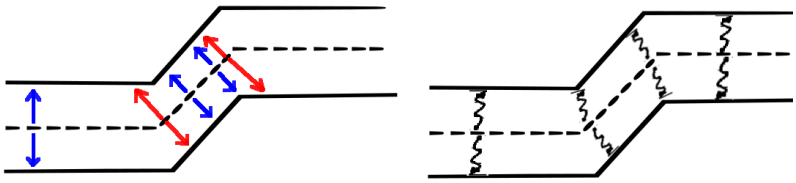

Figure 3.12: The rays (in red) spawned by the ray tracing approach (left) from the oblique mid-plane mesh elements do not intersect the correct elements in the surface. Only the blue colored rays intersect the correct elements in the surface. The nearest neighbor approach (right) behaves correctly.

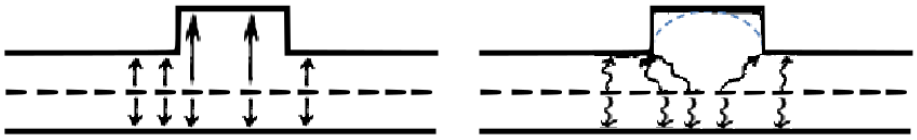

Figure 3.13: Although the nearest neighbor approach seems to solve the issue of the surface changing in unpredictable ways (Figure 3.12) it fails to estimate the correct thickness of some mid-plane elements (right). The ray tracing approach (left) behaves correctly.

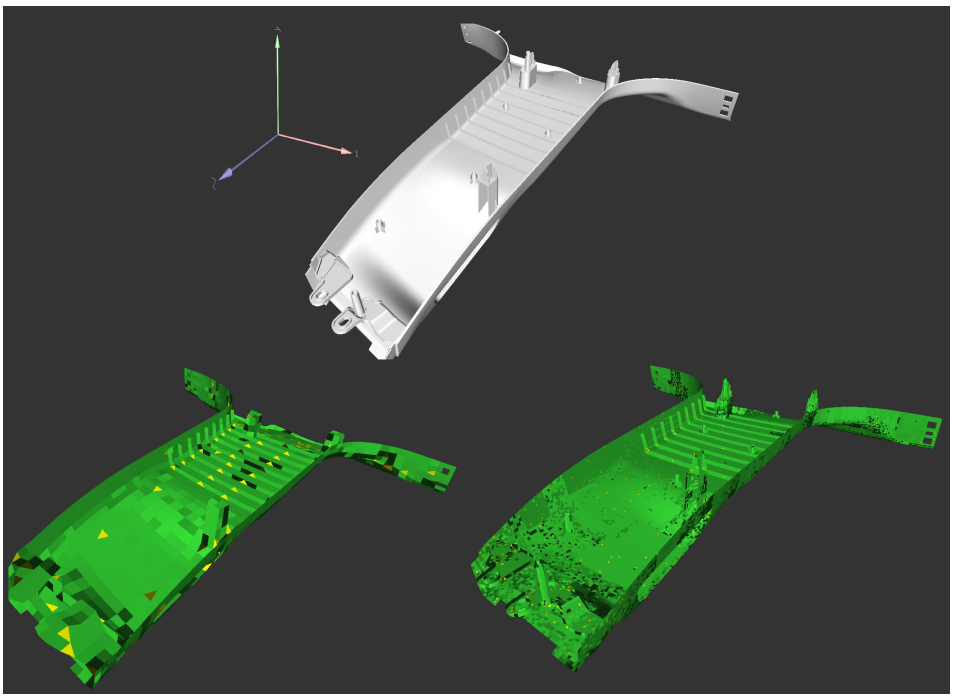

Figure 3.14: The B-Pillar Trim model (top) and the coarse (bottom left) and fine (bottom right) mid-plane meshes representations.

meshes, respectively. In order to ease the visualization and understanding of the results, some outliers were removed from the thickness values before

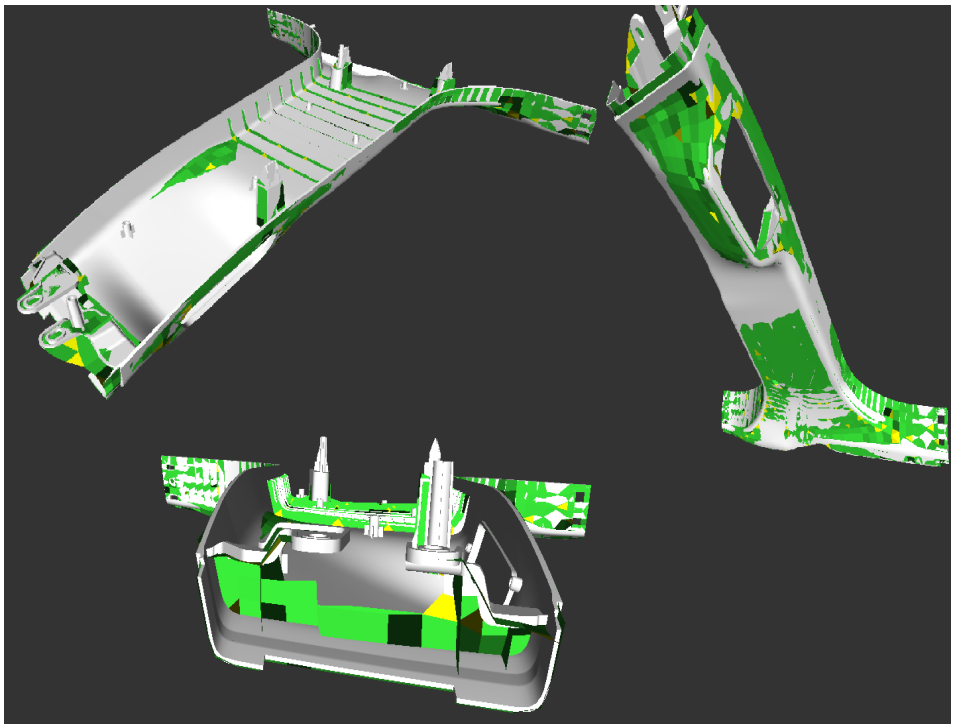

Figure 3.15: Ideally the mid-plane mesh should run inside the model surface, and hence not visible. However the coarse mid-plane mesh runs outside of the surface boundaries (the visible green regions).

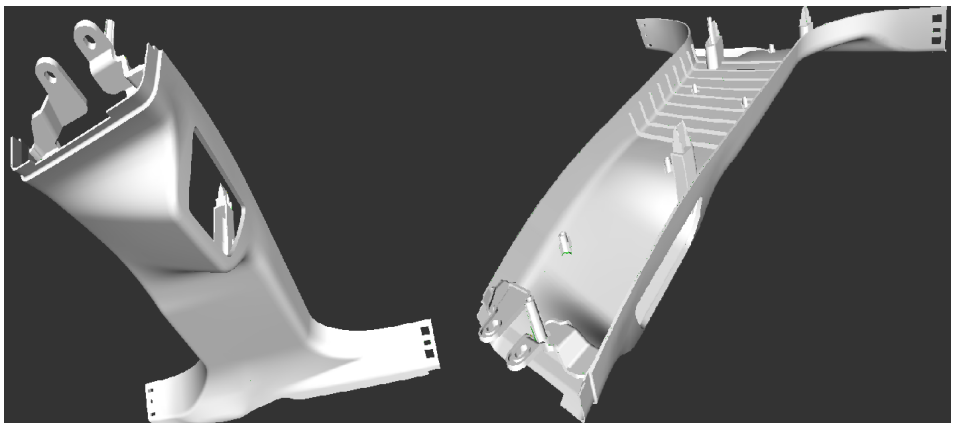

Figure 3.16: The fine mid-plane mesh is an accurate and detailed representation of the B-Pillar Trim. As the mesh runs inside the surface of the model it is not visible.

normalization. These outliers exhibited very large values that would compress all remaining results to a very thin range, compromising the graphics interpretation. It can be seen that for both mid-plane meshes, ray tracing estimate thicknesses of 0mm and thicknesses that are greater than the maximum thickness of the part (0.16mm).

For the nearest neighbor approach, figures 3.19 and 3.20 shows the thick-

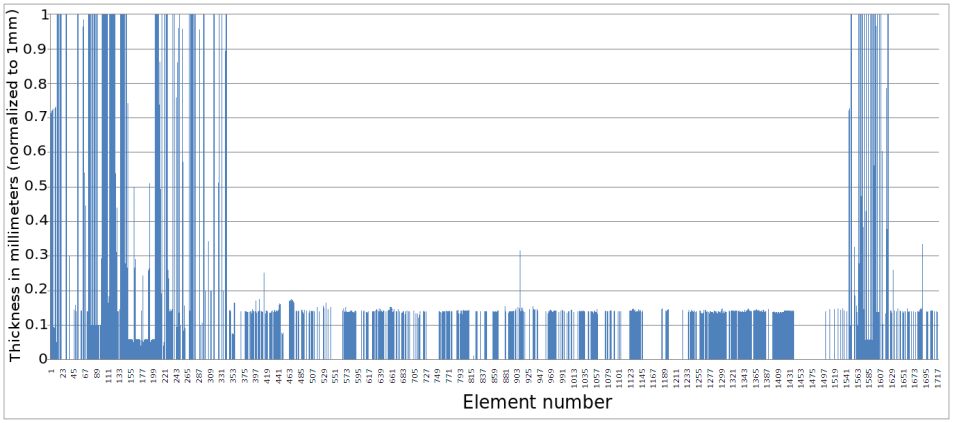

Figure 3.17: The thicknesses estimates (normalized) obtained with the ray tracing approach for the coarse mid-plane mesh representation of the B-Pillar Trim model.

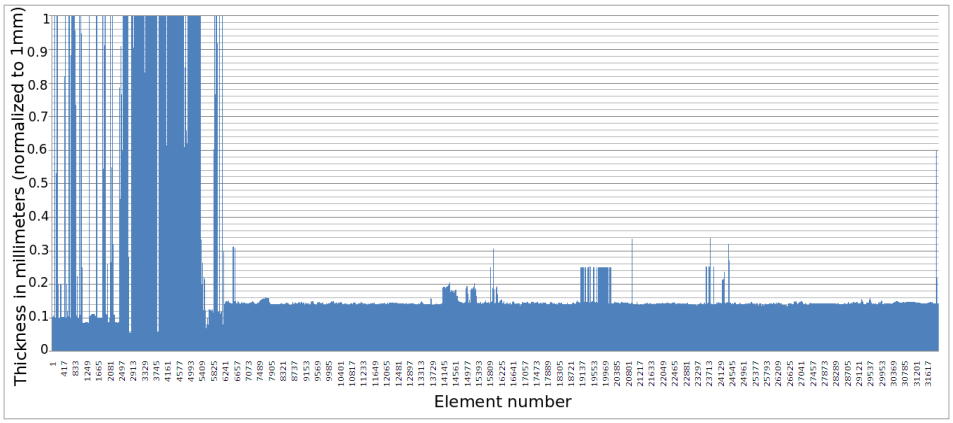

Figure 3.18: The thicknesses estimates (normalized) obtained with the ray tracing approach for the fine mid-plane mesh representation of the B-Pillar Trim model.

ness estimates (normalized to 1mm) obtained for the coarse and fine mid-plane meshes, respectively (again, with some outliers removed from the thickness values before normalization). Only for the coarse mid-plane mesh does nearest neighbor estimate thicknesses that are above the maximum thickness of the part, while for the fine mid-plane mesh representation the thicknesses estimates are very close to the real thicknesses.

With exception of the thicknesses estimated with the nearest neighbor approach for the fine mid-plane mesh, both approaches estimate thicknesses that do not seem correct or even reasonable. The reason of these inconsistencies is that it is assumed the mid-plane mesh runs inside the model's surface. However, as shown in figure 3.15 this is not true. With this in mind it is possible to identify why the approaches behave incorrectly. Figure 3.21 illustrates how the ray tracing approach behaves with one of the mid-plane elements that is outside (colored in blue). Two rays, one for each side of the mid-plane

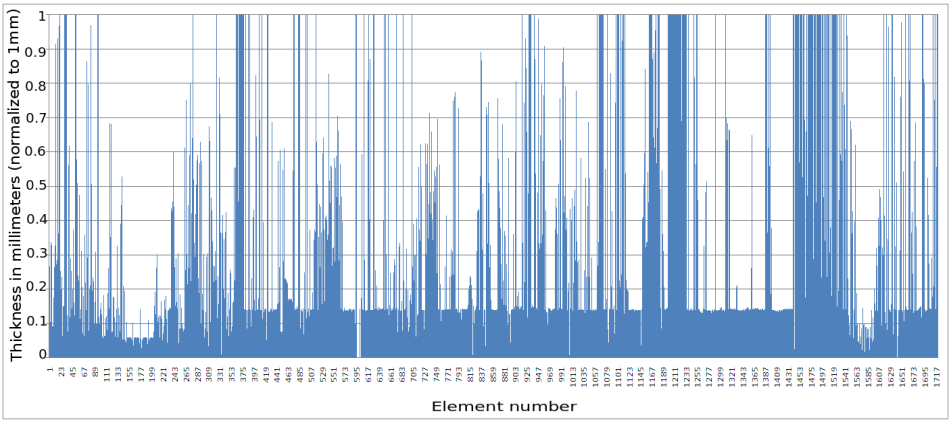

Figure 3.19: The thicknesses estimates (normalized) obtained with the nearest neighbor approach for the coarse mid-plane mesh representation of the B-Pillar Trim model.

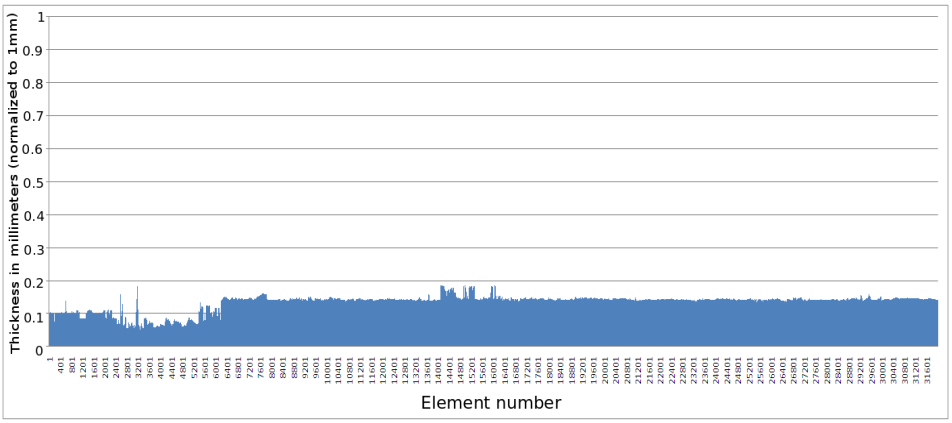

Figure 3.20: The thicknesses estimates (normalized) obtained with the nearest neighbor approach for the fine mid-plane mesh representation of the B-Pillar Trim model.

element are shoot in the direction of the white line path, intersecting two elements in the surface (colored in orange). Recall that the mid-plane mesh is a two dimensional abstraction of the model, and so, each mid-plane mesh element abstracts two elements of the surface, which ideally are the ones that are above and below it (Figure 3.4). Obviously, if the mid-plane mesh runs outside, then ray tracing will never intersect such elements in the surface, which will result in overestimated thicknesses.

A similar situation occurs with the nearest neighbor approach when the mid-plane mesh runs outside. Figure 3.22 shows the element of the surface (in purple) that is near to the blue mid-plane mesh element, which is outside. The distance between these elements, represented by the purple line, shows that something is wrong, as there are closer elements in the surface than the purple element. This can be explained by the shape of the surface, which is concave, and by the location of the blue mid-plane element, which is exactly

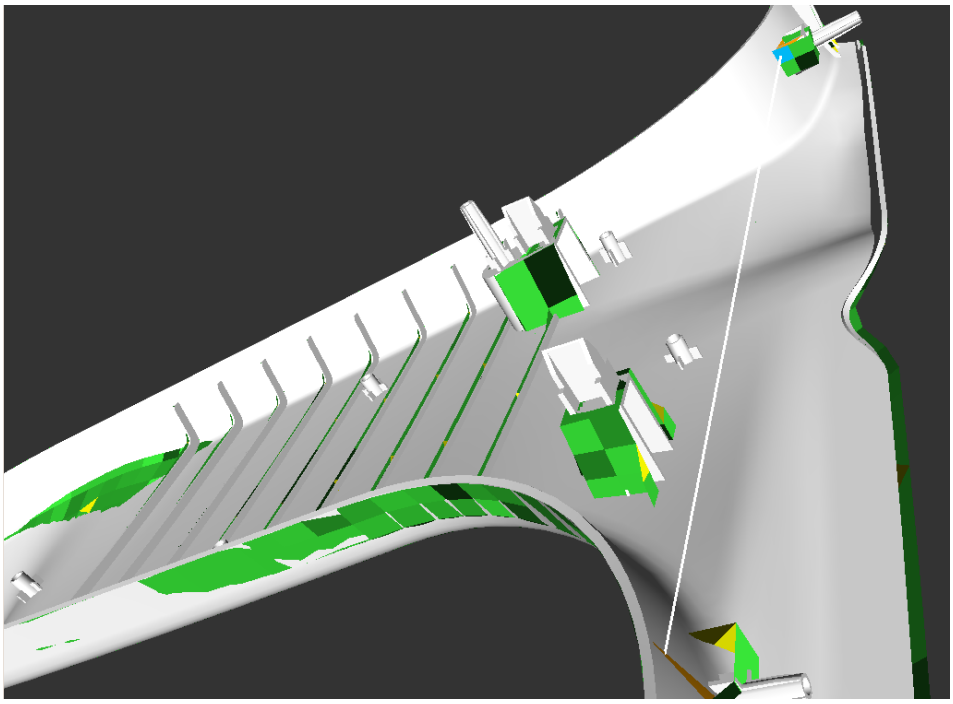

Figure 3.21: The B-Pillar Trim model and its mid-plane mesh representation. The rays (white line) shoot from the blue mid-plane element intersect elements in the surface colored in orange. As the mid-plane element is outside the boundaries of the model's surface, the orange elements in the surface are not the same elements that would be intersected if the mid-plane element was inside the boundaries of the model's surface.

at one of the extremes of the concavity. As the search for neighbors is limited to 90 degrees, only elements of the surface that are in the other extreme of the concavity are valid neighbors, reason why the "distant" purple element is the nearest one.

It should be easy, by now, to understand why ray tracing estimates thicknesses of 0mm. While some of the mid-plane elements that are outside shoot rays that intersect distant elements of the surface, others do not intersect elements at all. Figure 3.23 shows a region of the model's surface where several elements of the mid-plane mesh are outside. The white line represents the path that the rays shoot by one of these mid-plane elements (in blue) follow. Only for one side is an element of the surface intersected (in orange), for the other side the ray continues to infinity. It is then impossible to assign a thickness for these mid-plane elements, as ray tracing expects to find one intersection for each side of the mid-plane mesh element.

With the fine mid-plane mesh representation the nearest neighbor approach estimates thicknesses that are a reliable approximation of the real thicknesses. As the mid-plane mesh is an accurate and detailed representation of the model, the problems identified in figure 3.22 are avoided. However the improved accuracy and detail do not prevent the ray tracing approach

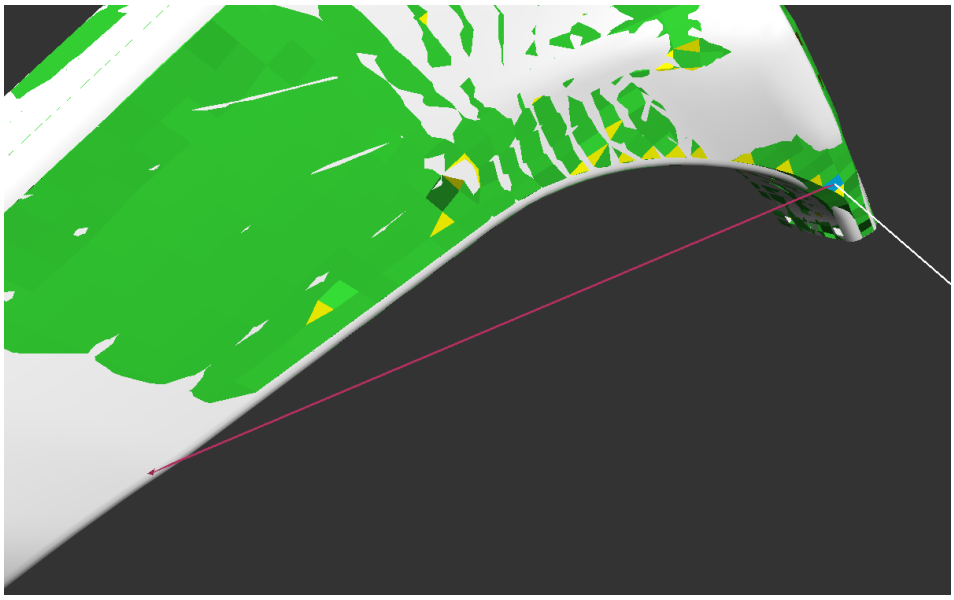

Figure 3.22: The B-Pillar Trim model and its mid-plane mesh representation. As the shape of the surface is concave and the search for neighbors is limited to 90 degrees, only elements of the surface that are in the other extreme of the concavity are valid neighbors. This explains why the "distant" purple element of the surface is the computed nearest neighbor of the blue mid-plane element.

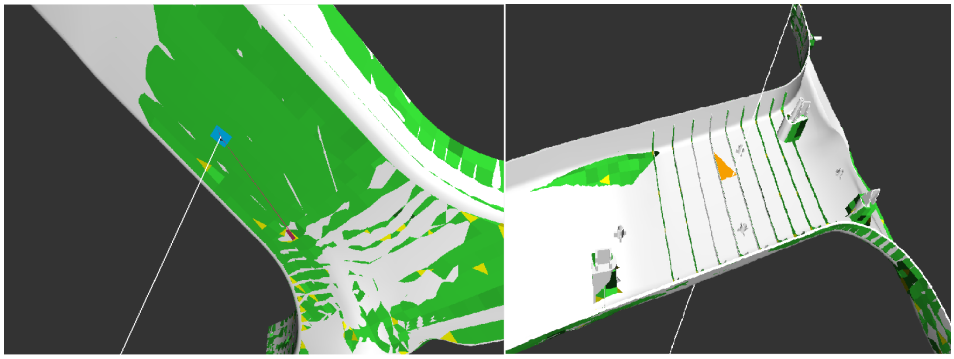

Figure 3.23: The B-Pillar Trim model and its mid-plane mesh representation. The rays shoot (white line) from the blue mid-plane element only intersect one element of the surface (the orange element on the right). Due to this, the ray tracing approach cannot assign a thickness to the blue mid-plane element.

from estimating thicknesses above the maximum thickness of the part. Figure 3.24 illustrates why ray tracing estimates such thicknesses. Although the blue mid-plane element is inside, the rays shoot follow the white line path, which runs inside the surface, not intersecting the surface elements of the rib. This is further illustrated in figure 3.25.

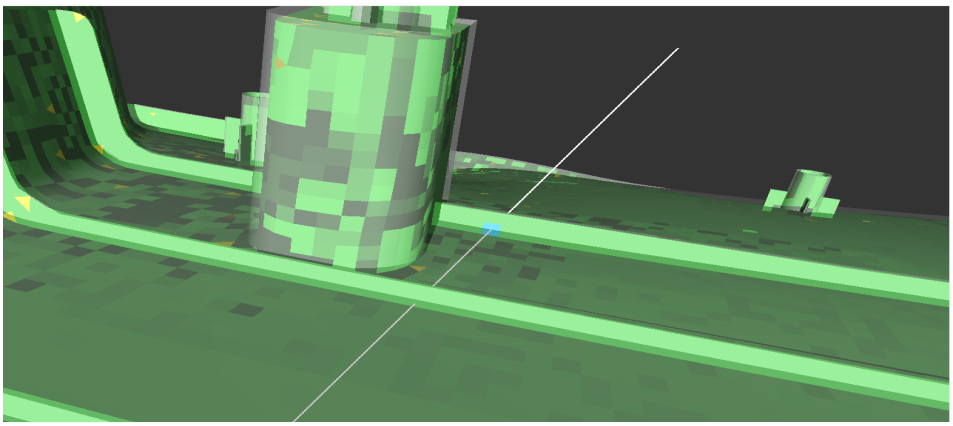

Figure 3.24: The B-Pillar Trim model (white translucent) and its fine mid-plane mesh representation. The blue mid-plane element shoots rays (white line) that run inside the surface, intersecting incorrect and distant elements of the surface.

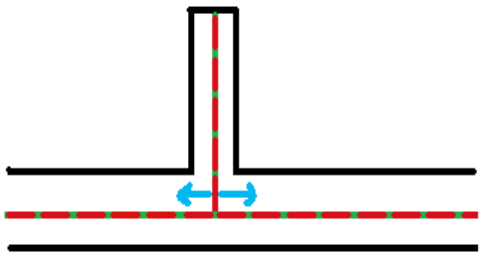

Figure 3.25: The black lines represent the B-Pillar Trim model surface, the red line represents the mid-plane mesh representation and the green lines represent the individual mid-plane elements. The blue arrows indicate the directions of the rays shoot from the mid-plane element, which run inside the surface, hence not intersection the correct surface elements.

3.4.1 Some conclusions on the behavior of the approaches

The tests performed so far allow to conclude that the behavior of each approach is not only determined by the accuracy and level of detail of the mid-plane mesh representation, but also, by the geometric configuration of the model.

The ray tracing approach fails to estimate accurate thicknesses when "sudden" changes in the shape of the surface occurs, or when ribs are present. The nearest neighbor approach "smooths" local thickness variations, although this was not verified with the fine mid-plane mesh representation of the B-Pillar Trim. And, when subject to coarse mid-plane meshes, both approaches estimate thicknesses above the maximum thickness of the model, with ray tracing even estimating thicknesses of 0mm.

It can be concluded that both approaches fail to estimate the accurate thicknesses when subjected to certain geometric configurations. Also the thickness estimates obtained when using accurate and detailed mid-plane meshes achieve more reliable results than with the inaccurate or poorly detailed ones. It is then mandatory to understand in what geometric configurations the approaches behave incorrectly and when the mid-plane mesh is inaccurate and poorly detailed, so it becomes possible to take the proper measures. In chapter 4 a systematic quantitative analysis of the accuracy of both approaches is presented, as well as a thorough identification of particular geometric configurations under which their accuracy can be compromised.

Chapter 4

Quantitative analysis

Chapter 3 presented two approaches for thickness estimation. However, both approaches produced inaccurate thickness estimates when some particular conditions occur. These conditions can be classified in two groups, which are detailed below:

1. **the part's geometry is not accurately captured by the mid-plane mesh** - the mid-plane mesh is a coarse representation of the part's geometry; its goal is to be used on finite elements simulations of the part's structural characteristics. This coarseness implies that some of the part's details are not captured by the mid-plane mesh and that in some cases the mesh is outside the part's volume. This error is illustrated in figures 4.1 - the drawings correspond to the schematic depiction of 4 virtual test specimens supplied by FORD in order to analyze this particular case.

2. **ribs** - In a rib the mid-plane mesh, running inside the rib, will have normals which are perpendicular to the surface main orientation. On the junction between the rib and the surface rays will be shot inside the surface, thus failing to estimate thickness accurately. Figures 4.2 depict three such cases where the RT algorithm produces very bad estimates - as before these correspond to schematic drawing of virtual test specimens supplied by FORD.

Correctly handling such cases requires a systematic quantitative analysis of the proposed approaches behavior and accuracy. Analysis of the approaches accuracy with real car parts is difficult because the exact local thicknesses are unknown. In order to enable such analysis seven simple virtual test specimens, whose exact thickness is known (3 mm for all parts), were modeled and used throughout the whole validation process. For each specimen three different mid-plane meshes were supplied, corresponding to different meshing granularities: each element on each mid plane mesh has edges with length 8mm, 5mm or 2mm. This allows studying the thickness estimate accuracy

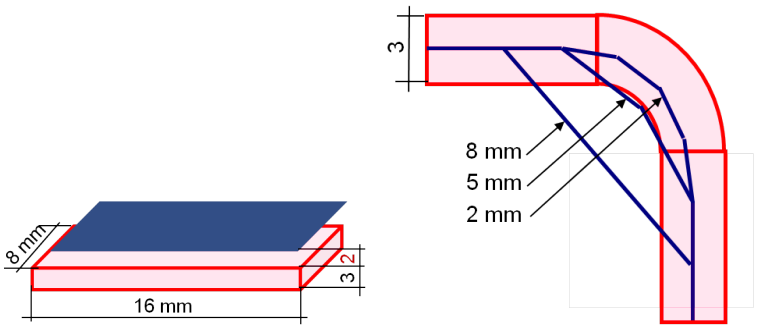

(a) **Specimen 1**: mid-plane mesh completely outside the specimen's volume

(b) **Specimen 2**: mid-plane mesh misses the surface details depending on its coarseness

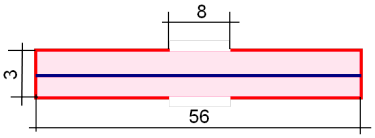

(c) **Specimen 3**: holes in the specimen surface are not represented on the mid-plane mesh

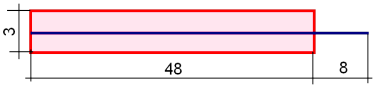

(d) **Specimen 4**: the mid-plane mesh extends outside the specimen's volume

Figure 4.1: Virtual specimens - Inaccurate mid-plane meshes (colored in blue)

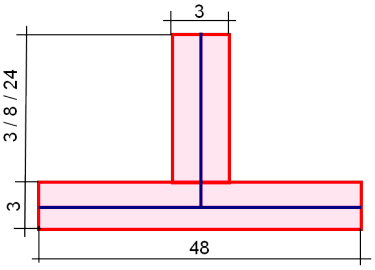

(a) Specimen 5

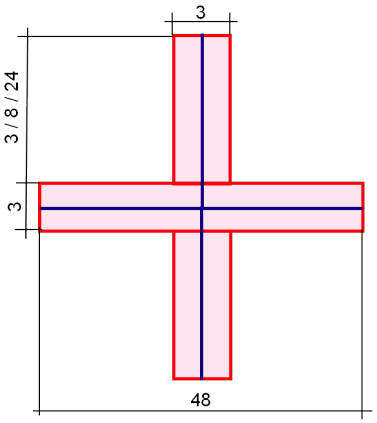

(b) Specimen 6

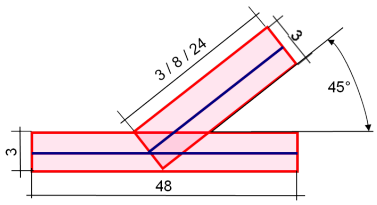

(c) Specimen 7

Figure 4.2: Virtual test specimens - Ribs (mid-plane meshes colored in blue)

for different representations. Figure 4.3 presents these specimens with the 2 mm mesh, except for specimen 2, where both the 8 mm and the 2 mm meshes are shown (figures 4.3(b) and 4.3(c), respectively). These specimens stress

particular situations where the approaches are expected to fail. Specimens 1 to 4 (except specimen 2 with 2mm mesh) have the mid-plane mesh either total or partially outside the specimen's surface, specimens 5 to 7 include ribs - thickness is not exactly defined at the regions where the rib intersects the main surface.

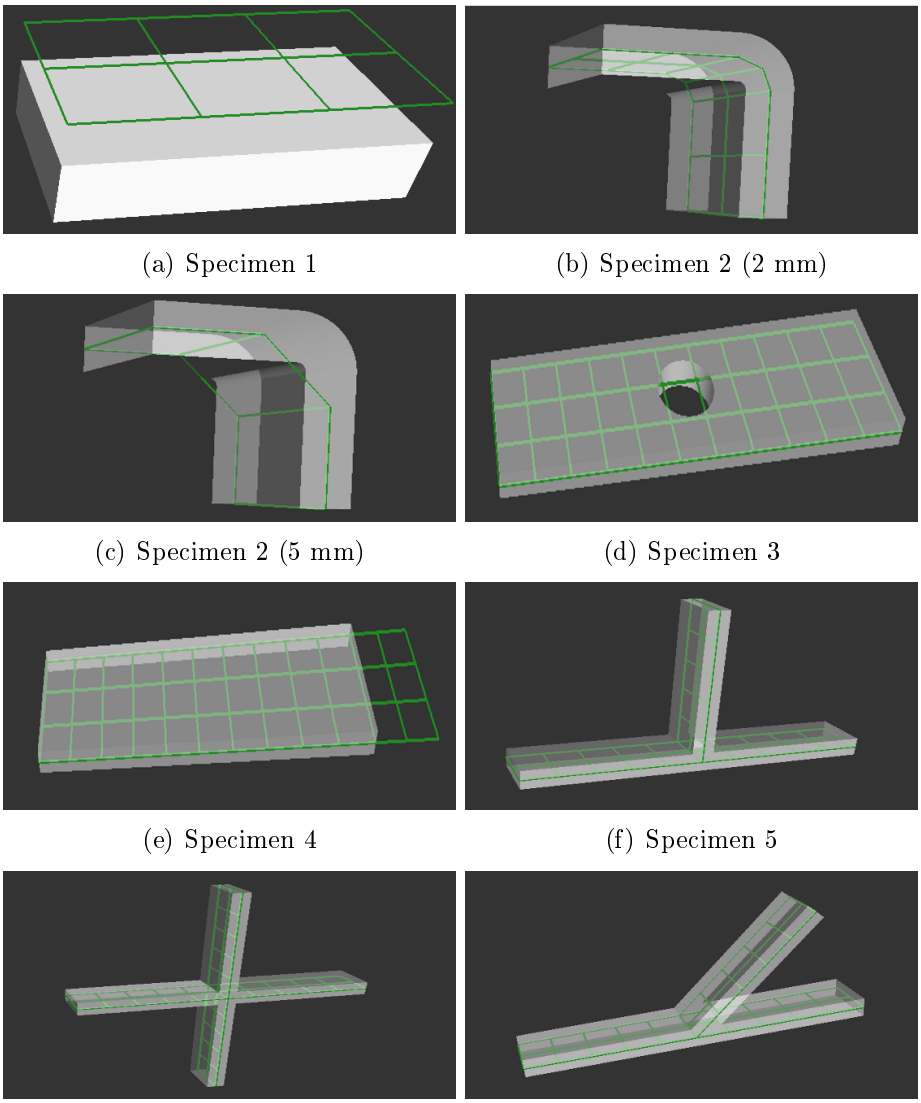

(a) Specimen 1 (b) Specimen 2 (2 mm)

(c) Specimen 2 (5 mm) (d) Specimen 3

(e) Specimen 4 (f) Specimen 5

(g) Specimen 6 (h) Specimen 7

Figure 4.3: Virtual test specimens used for quantitative analysis of the thickness estimate accuracy (All specimens have constant 3 mm thickness).

4.1 Metrics for quantitative analysis

Knowledge of the exact thickness of the specimens allows for a quantitative analysis of the thickness estimation process. This analysis requires selecting metrics that can be used as objective functions. Two such metrics are used

throughout this chapter: the arithmetic mean and the root mean square error. The objective function is RMSE, which must be minimized.

Arithmetic Mean (AM) - since the actual thickness is a constant (and equal to 3mm) across the whole surface for all the specimens, the arithmetic mean $\bar{T}$, calculated as the average of the estimated thickness, $\tilde{T}_i$, across all N elements of the mid-plane mesh (see equation 4.1), gives a fast hint of whether or not the estimation process is converging towards the correct value. It is a global metric, however, thus it does not capture whether there are local errors on the estimates that can be smoothed away by the averaging process. Furthermore, it would not convey useful information if the real thickness varied from element to element.

$$\bar{T} = \frac{1}{N} \sum_{i=1}^{N} \tilde{T}_i \tag{4.1}$$

Root Mean Square Error (RMSE) - RMSE takes the square of the individual differences, also called residuals, between the estimated and the real thickness at each element of the mid-plane mesh and aggregates them onto a single metric that has predictive power and is perceived as a good measure of accuracy [DeG80] (equation 4.2). The lower the RMSE the better the thickness estimates produced by the associated algorithm. RMSE heavily weights outliers (i.e., particularly bad local estimates) due to the squaring of the residuals, whereas small residuals are attributed very small weights; it is felt, however, that for Finite Element Analysis of structural properties outliers can strongly affect the simulation result, thus this is a desirable property.

$$RMSE = \sqrt{\frac{\sum_{i=1}^{N} (\tilde{T}_i - T_i)^2}{N}} \tag{4.2}$$

4.2 Results Analysis

Results for the seven specimens, with three different mid-plane mesh resolutions (2, 5 and 8 mm) and for two approaches, are presented in table 4.1.

In those cases where the mid-plane mesh runs outside the specimen's surface (specimens 1 to 4) both approaches fail to find valid points on both sides of the mesh and, consequently, fail to estimate the thickness. Figures 4.4(a) and 4.4(b) illustrate this for specimen 3. The hole prevents the approaches from finding valid points on the specimen's surface. The particular values presented at table 4.1 for specimens 1 to 4 result from the fact that an estimate $\tilde{T}_i$ equal to zero was generated for these cases; this is particularly evident for specimen 1 where estimates could not be generated for any element since all of them are outside the specimen, thus resulting on $\bar{T} = 0.0$. The fact that the mid-plane mesh is outside the specimen's surface means that it is not a

		Ray tracing		Nearest Neighbor	
		$\bar{T}$	RMSE	$\bar{T}$	RMSE
Specimen 1	2 mm	0.0000	3.0000	0.0000	3.0000
	5 mm	0.0000	3.0000	0.0000	3.0000
	8 mm	0.0000	3.0000	0.0000	3.0000
Specimen 2	2 mm	3.0004	0.0026	2.6487	0.5066
	5 mm	2.9998	0.0015	2.9991	0.0026
	8 mm	2.0000	1.7321	3.1214	0.2101
Specimen 3	2 mm	2.8259	0.7227	2.7329	0.6110
	5 mm	2.9091	0.5222	3.0889	0.8830
	8 mm	3.0000	0.0000	2.6222	0.9994
Specimen 4	2 mm	2.5714	1.1339	3.5828	2.5938
	5 mm	2.5000	1.2247	3.8609	2.6487
	8 mm	2.5714	1.1339	3.7385	1.9544
Specimen 5	2 mm	5.5000	9.1856	2.6856	0.4855
	5 mm	3.0000	0.0000	2.9999	0.0001
	8 mm	3.0000	0.0000	2.9999	0.0001
Specimen 6	2 mm	6.7500	12.9903	2.7352	0.4242
	5 mm	3.0000	0.0000	3.0001	0.0001
	8 mm	3.0000	0.0000	3.0001	0.0001
Specimen 7	2 mm	3.2914	0.9356	2.6595	0.5376
	5 mm	3.4030	1.1037	3.0578	0.1583
	8 mm	3.0000	0.0000	3.0000	0.0000

Table 4.1: Results for the thickness estimation approaches.

good representation of the original specimen; these situations will be handled explicitly (see chapter 5).

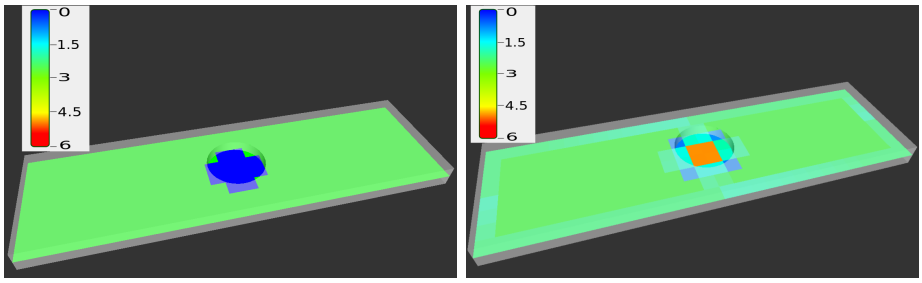

(a) Specimen 3 - Ray tracing. (b) Specimen 3 - Nearest neighbor.

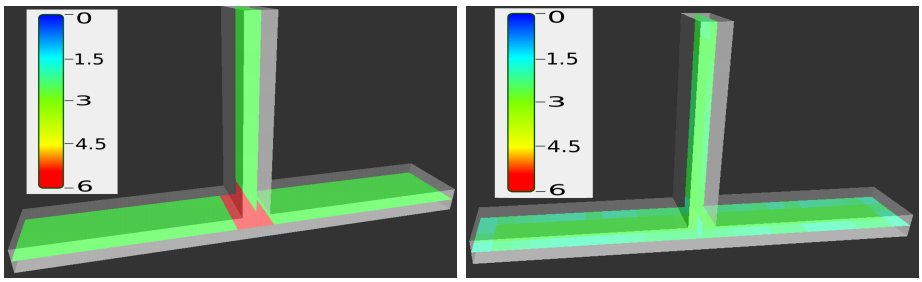

(c) Specimen 5 - Ray tracing. (d) Specimen 5 - Nearest neighbor.

Figure 4.4: Thickness estimation within holes and near ribs - pseudo color maps.

Specimens 5 to 7 illustrate situations where ribs are present. It is evident that the ray tracing approach fails when the midplane mesh element's centroid is aligned with the rib - rays, which are shot along the element's normal, will run inside the specimen, finding an intersection at distant points of the specimen's surface and overestimating thickness (figure 4.5(a)). This is particularly evident for the finer granularity meshes. The nearest neighbor approach does not suffer from this problem. It will still be able to find nearest points near the rib's junction with the specimen's surface, thus avoiding large thickness estimation errors (figure 4.5(b)). Figures 4.4(c) and 4.4(d) clearly show that the nearest neighbor approach outperforms ray tracing at these particular regions.

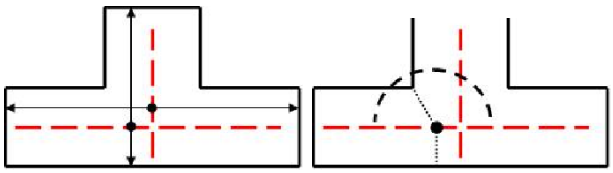

(a) Ray tracing. (b) Nearest neighbor.

Figure 4.5: Thickness estimation near ribs. Black lines represent the specimen's geometry, whereas the red dashed line represents the mid-plane mesh.

Table 4.1 also shows a somehow surprising result: the error of the nearest

neighbor approach tends to increase as the mesh granularity becomes finer. Figures 4.4(b) and 4.4(d) illustrate why. When searching for the nearest point in the specimen's surface, the elements that are close to the mesh boundaries find the specimen's lateral surface as its closest neighbor (see figure 4.6). The thickness estimate is thus smoothed and will diverge from its actual value, suggesting a round edge. A solution for this divergence, which occurs with most parts, is discussed in section 4.3.2.

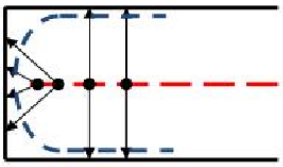

Figure 4.6: Divergence of the nearest neighbor approach close to the mid-plane mesh boundaries.

Summarizing, both approaches produce wrong thickness estimates when the mid-plane mesh is a very inaccurate approximation of the part's geometry and runs outside it - a technique will have to be developed to handle these cases explicitly. Additionally, the ray tracing approach overestimates thickness in the presence of ribs, whereas the nearest neighbor approach underestimates thickness near the mid-plane mesh boundaries.

4.3 Approaches behavior improvement

4.3.1 Inaccurate mid-plane meshes

The coarser the granularity of the mid-plane mesh the worst its accuracy as an approximation of the part's geometry. Often, this results on the mid-plane mesh running outside the part's surface, which leads to thickness estimation errors, as shown in the previous section. Two different cases occur with this inaccurate representation of the part's geometry: either the mesh is outside the surface but it still encompasses the part's geometry (virtual specimens 1 and 2, figures 4.3(a) and 4.3(c)), or the mesh runs outside the surface but this does not correspond to any region of the part's geometry (virtual specimens 3 and 4, figures 4.3(d) and 4.3(e)). Detecting whether an element's centroid is contained within the part's volume is a generalization of the well-known point in polygon problem and can be solved by resorting to ray tracing: if a ray is shot from a given point along any direction, that point is inside the closed surface if it intersects the surface an odd number of times, else it is outside the closed surface [VHK+90]. Thus, for each centroid, one ray is shot along the element's normal direction for each side of the element. If each of these rays intersects the surface an odd number of times, then the centroid is inside the part. If both rays intersect the surface an even number of times,

then the centroid is outside the surface. In this latter case, and if at least one of the rays intersects the surface more than zero times, the side of the centroid whose ray reported the closest intersection is selected as the one closest to the surface and thickness is estimated as the difference between the two closest intersections of that ray. This process is depicted in figure 4.7. The part's surface is represented by the solid black lines, the mid-plane mesh is depicted by the dashed red line and the rays correspond to the blue arrows. The brackets represent the estimated thicknesses by subtracting the distances found by the two closest intersections along the same ray.

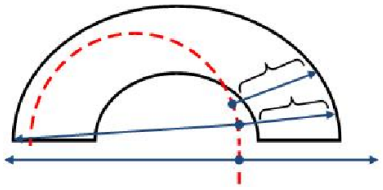

Figure 4.7: Detection of whether the mid-plane mesh is outside the part's surface.

Specimens 1 and 2 with 8 mm meshes illustrate two cases where the mid-plane mesh is outside the part's surface but still encompasses it. By detecting whether each element's centroid is outside the part the exact thickness is found and a RMSE equal to zero is obtained (figure 4.8).

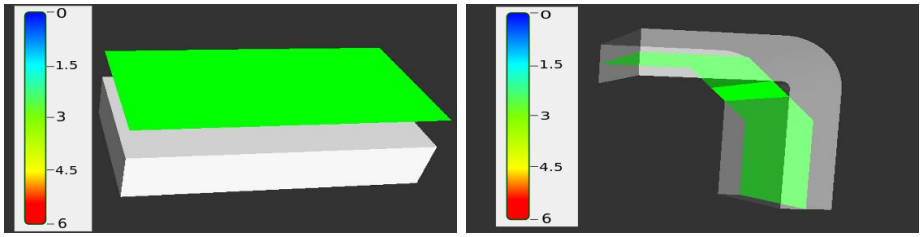

(a) Specimen 1. (b) Specimen 2.

Figure 4.8: Virtual specimens 1 and 2 with ray tracing corrected thickness estimation - pseudo color.

The effectiveness of the ray tracing corrected thickness estimation is also shown with a real part representing a B-Pillar Trim, whose majority of the mid-plane elements is outside the part's surface, as illustrated in figure 4.9. Figure 4.10 shows thickness estimations obtained with ray tracing and nearest neighbor (left and center) and with the detection of elements outside the part's surface (right).

However, for some elements of the mid-plane mesh no intersections are found on either side of the element, as illustrated in the bottom part of figure 4.7. This happens within the hole of specimen 3 and on specimen 4 on the region of the mesh that extends further than the specimen's surface. Such elements are handled explicitly in chapter 5.

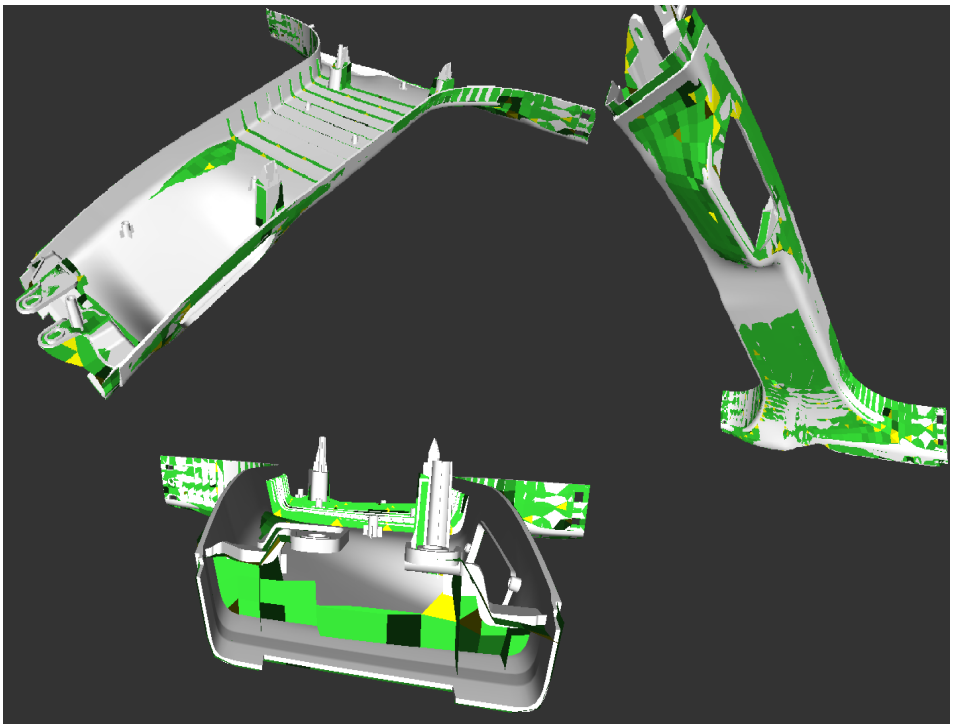

Figure 4.9: Ideally the mid-plane mesh should run inside the digital model surface, however the coarse mid-plane mesh runs outside of its boundaries.

4.3.2 Nearest neighbor divergence

In order to limit the divergence occurring near the mid-plane mesh boundaries with the nearest neighbor approach, a limitation has been imposed on the maximum acceptable angle between the element's normal and the direction defined by the element's centroid and the surface nearest point. By limiting this angle it is expected that the part's lateral surface is rejected as a nearest neighbor, thus forcing the algorithm to expand its search onto regions of the surface that are farther away from the mid-plane element 4.11.

This technique requires some precaution. Some real parts' geometries are modeled with polygons that have an area orders of magnitude larger than the respective mid-plane elements area. If the limitation of the angle is too strict, then some mid-plane elements could reject the surface polygon, missing the correct nearest neighbor and overestimating local thickness. In the presence of ribs the angle rejection technique might also reject the correct nearest neighbor, resulting in overestimating thickness. The occurrence of these two cases depends on the geometric configuration of the part's surface and on the threshold applied to the angle. To study the impact of this technique three different angle thresholds have been tested: 80, 65 and 45 degrees.

Table 4.2 presents the RMSE obtained for 4 different specimens and respective fine grained midplane meshes (2 mm). For these specimens a threshold of 45° produces the smaller RMSE. However, for complex real parts such a large

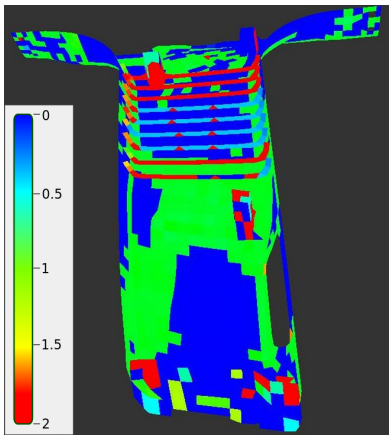

(a) Ray Tracing.

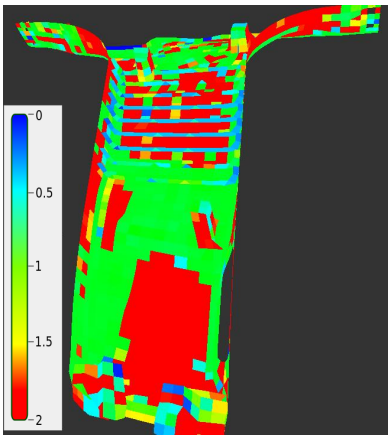

(b) Nearest Neighbor.

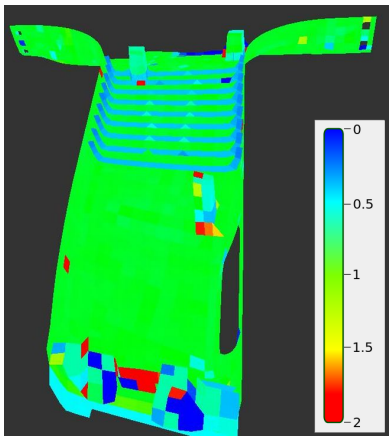

(c) RT corrected.

Figure 4.10: Thickness estimation (the values were scaled to the interval of 0mm to 2mm due to confidential issues) for the B-Pillar Trim - pseudo color.

threshold results in many rejections and, consequently, in many local errors (see figure 4.12, where significantly wrong thickness estimates are highlighted in red). A threshold of 80° does not induce such errors and still its impact on the RMSE is significant, more than halving it.

4.4 Conclusion

Results obtained using each approach individually (table 4.1) allowed the identification of three different situations that lead to poor thickness estimation as measured by RMSE: the mid-plane mesh runs outside the part's surface preventing the proposed approaches to find valid points on the part's surface, the nearest neighbor approach diverges on the mid-plane boundaries and the ray tracing approach fails to find accurate thicknesses on ribs.

The first problem was addressed by using ray tracing to detect whether

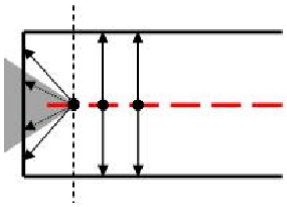

Figure 4.11: Limiting acceptable angle for nearest neighbor: the gray triangle represents the unacceptable angle domain, dashed arrows represent rejected nearest point directions, solid arrows represent accepted directions.

	Specimen 2	Specimen 5	Specimen 6	Specimen 7
RT	0.0026	9.1856	12.9903	0.9356
NN (no limit)	0.5066	0.4855	0.4242	0.5376
NN (80°)	0.2581	0.2223	0.2112	0.2546
NN (65°)	0.0819	0.1384	0.1343	0.1733
NN (45°)	0.0197	0.0356	0.0491	0.1481

Table 4.2: RMSE results for nearest neighbor angle limitation with 2mm midplane meshes.

an element's centroid is outside the surface. In such cases the difference between the two closest intersections detected on the same side of the element is used as thickness estimation. There are still some elements where no intersections are found on either side: these are tagged as "Incorrect" for manual post-processing. The divergence with the nearest neighbor approach near the mid-plane mesh boundaries was minimized by limiting the maximum angle allowed between the element's normal and the direction defined by the element's centroid and the nearest point on the part's surface. By requiring that this angle is less than 80° RMSE was significantly reduced while avoiding other geometric errors. The ribs inaccuracies associated with the ray tracing approach were not addressed explicitly since these are completely avoided by the nearest neighbor approach.

The above results suggest that:

- nearest neighbor fails on the mid-plane mesh boundaries but ray tracing provides good estimates at these locations. The heuristic of limiting the angle reduces RMSE, but does not allow estimates as good as ray tracing; this is corroborated by the results achieved with part 2 (table 4.2);
- ray tracing fails on ribs, but nearest neighbor provides good estimates at these locations.

Both approaches complement each other: if each approach's best estimate can be selected for each element of the mid-plane mesh then RMSE is reduced.

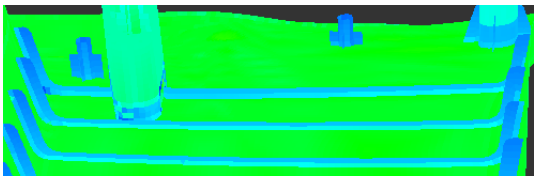

(a) No angle threshold.

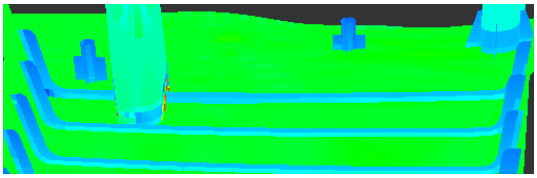

(b) 80° threshold.

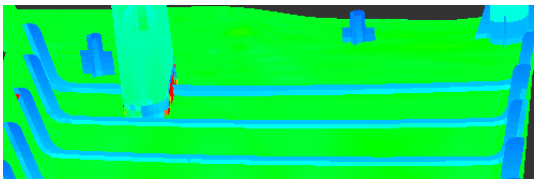

(c) 65° threshold.

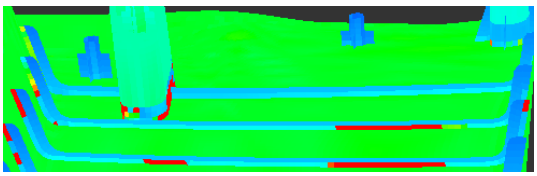

(d) 45° threshold.

Figure 4.12: Wrong thickness estimates induced by limiting the maximum acceptable nearest neighbor angle (highlighted in red).

Figure 4.13 illustrates this approach for part 5: for each mid-plane element the estimate that minimizes the difference to the correct thickness was manually selected from the RT and NN with 80° limitation algorithms. The final result is a very good overall estimate of the part's thickness, with an average mean of 3.0091 and RMSE equal to 0.0325. Small errors are visible only on the mid plane mesh boundaries on the rib joint with the part's main body, since these are the locations where both approaches induce some inaccuracy.

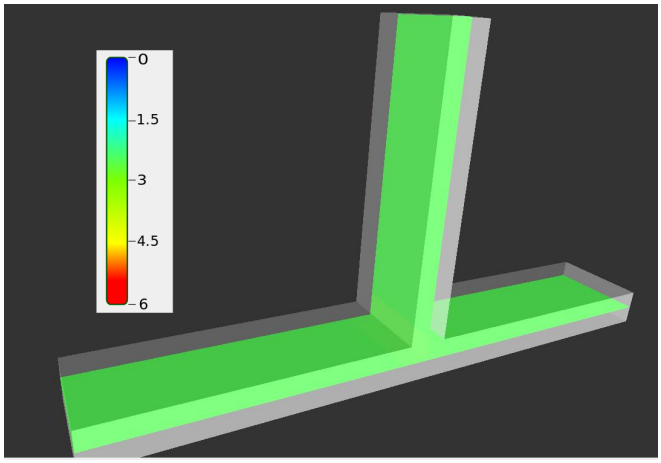

Figure 4.13: Best estimate from either ray tracing or nearest neighbor manually selected for each mid-plane mesh element - pseudo color.

Chapter 5

Thickness estimation improvement

5.1 Method For Thickness Accuracy Improvement (MFTAI)

5.1.1 Introduction

In chapter 4 a thorough study of the approaches was performed in order to quantitatively assess their accuracy. The analysis carried out on the virtual test specimens allowed, not only to identify the situations that lead to inaccurate thickness estimations, but also to suggest two methods for improving the accuracy of the approaches: using ray tracing to detect whether an element's centroid is outside the part's surface, computing, in such cases, the thickness as the difference between the two closest intersections detected on the same side; and limiting the search angle of the nearest neighbor approach. The analysis ended with the important conclusion that both approaches complement each other, suggesting that if a criterion can be found that allows automatic selection of either the RT or the NN estimate for each element, then RMSE can be significantly reduced and the whole results would be much more reliable from the FEA simulation process point of view.

Such a criterion is not evident however, due to the complexity of real world parts. Real geometries and mid-plane meshes have lots of details and particular configurations that make it very difficult to establish which is the best estimate - particularly, the real local thicknesses are not known, since this is exactly the quantity that is being measured. Analysis of the local geometries in order to identify features and/or mid-plane mesh boundaries may also reveal too complex to be performed accurately and would add significant complexity to the CAD2FE tool, as a database of features would need to be maintained [HPR00].

It is then necessary to develop a method that can decide which approach will estimate the most accurate thickness for a particular mid-plane element. However, even with this combined approach, there are still situations where the accuracy of the thickness estimates is compromised. For example, the combined approach may use ray tracing to detect if an element is outside the model's surface, but, either approach may fail to estimate an accurate thickness (figure 5.1). So, ideally, the method should be able to assess if one of the approaches can estimate an accurate thickness, deciding which approach to use in such cases. Otherwise the method should tag the element somehow, for post-processing.

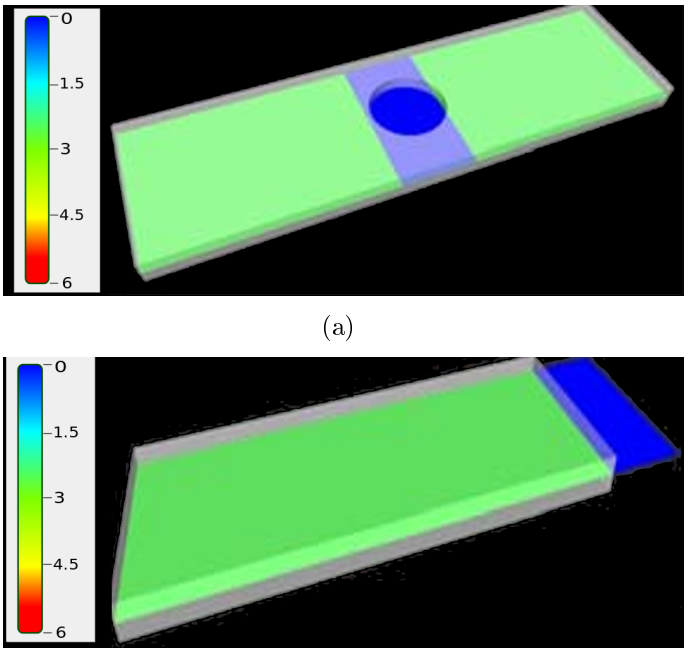

(a)

(b)

Figure 5.1: Even with the combined approach, some mid-plane elements have inaccurate thicknesses (blue colored regions) - pseudo color.

Basic Premise - Detection

A common characteristic of both approaches, despite the difference in their behavior, is that both estimate virtually the same thicknesses when the mid-plane mesh is accurate and detailed. Figures 5.2 and 5.3 illustrates this situation: the pseudo color-map of thicknesses show same color zones that are shared by both approaches.

With this assumption the approaches can be modified so they both estimate the thickness, comparing the estimates to detect "inconsistencies". These "inconsistencies" can be defined as elements whose difference between the thickness estimated by each approach exceeds a certain threshold, or when ray tracing detects that a mid-plane element is outside the boundaries

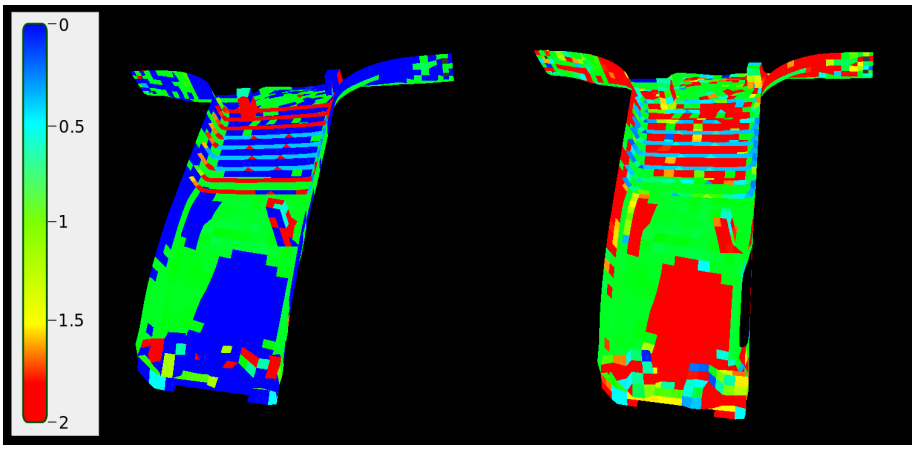

Figure 5.2: Pseudo color-map of ray tracing (left) and nearest neighbors (right) thickness values (the values of thickness were scaled to a range of 0mm to 2mm due to confidential issues). Blue and red colored regions indicate inaccurate thicknesess, while the green colored region indicates accurate thicknesses.

of the surface. Armed with this way of identifying inconsistent elements, it is necessary to define how the accuracy of their thicknesses can be improved.

Basic Premise - Correction

One important property of thermoplastic injection molded parts is that it can state that thickness should not vary sharply from one element to a neighbor one. It is then feasible to use the information about the neighborhood of an inconsistent mid-plane element in order to assess if the local thickness accuracy can be improved. With this, a method for thickness accuracy improvement (MFTAI) based in the concepts of propagation and neighborhood is proposed. Its basic premise is to tag elements whose information collected by each approach suggests it may be inconsistent, and post-process these elements, using the neighboring information to improve the accuracy of the estimates of thickness.

Figure 5.4 shows the UML diagram that illustrates how the MFTAI changes the overall behavior and data flow of the CAD2FE tool, allowing to assess when the approaches accuracy is compromised and to post-process these cases: In the stage of thickness estimation a new activity, which will be defined in the next section, detects and tags inconsistencies in the thickness accuracy estimates; this information can be then collected by the new stage, MFTAI, for improving the accuracy of these mid-plane elements.

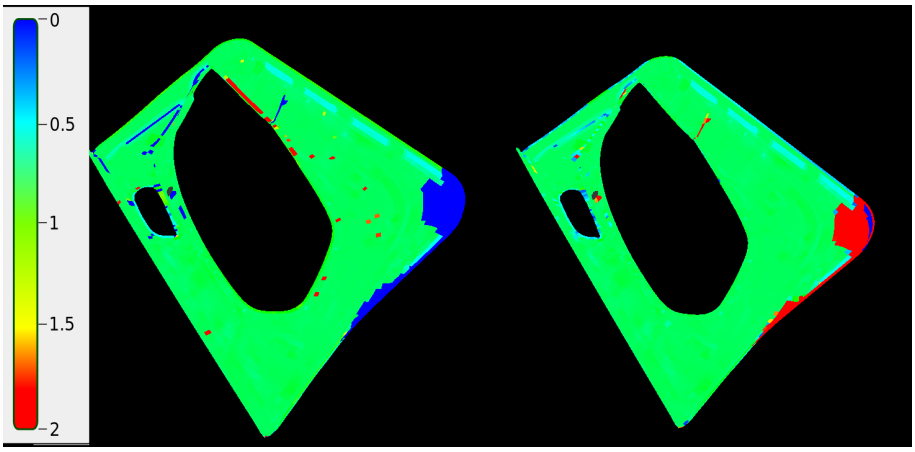

Figure 5.3: Pseudo color-map of ray tracing (left) and nearest neighbors (right) thickness values (the values of thickness were scaled to a range of 0mm to 2mm due to confidential issues). Blue and red colored regions indicate inaccurate thicknesess, while the green colored region indicates accurate thicknesses.

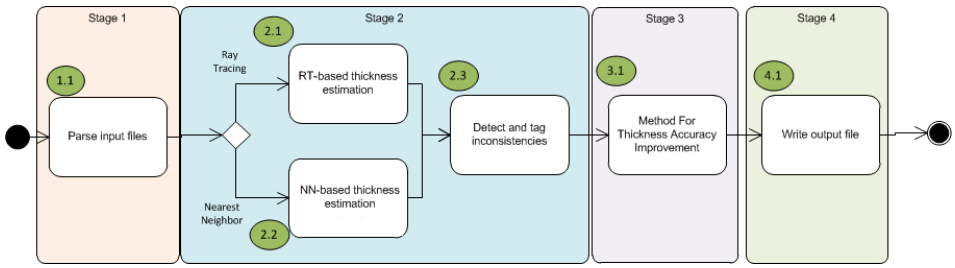

Figure 5.4: UML activity diagram. The diagram illustrates the behavior and overall data flow of the CAD2FE tool.

5.1.2 Method's Heuristics

In order to understand in detail the behavior of MFTAI, it is necessary to have an understanding of its two basis concepts: propagation and neighborhood. If one observes the MFTAI as a black box, the concept of propagation explains how it works. Basically, the MFTAI propagates the thickness of correct (the best possible estimate) thickness elements to incorrect thickness elements. How this propagation is performed is defined by the concept of neighborhood: when two elements are directly connected in Euclidean space, i.e., they share a vertex, they are classified as neighbors. The propagation of thickness can then only occur when two elements are neighbors. However, since the part's surface can contain several ribs, bosses, etc (figure 5.5), that may have different values of thickness, it is necessary to avoid propagating the thickness among these. To achieve this, the concept of neighborhood is reinforced by the notion of direct neighbors: Two elements that are neighbors are classified as direct neighbors if the angle formed by their normals is less than a given threshold (25^{o}- see section 5.2).

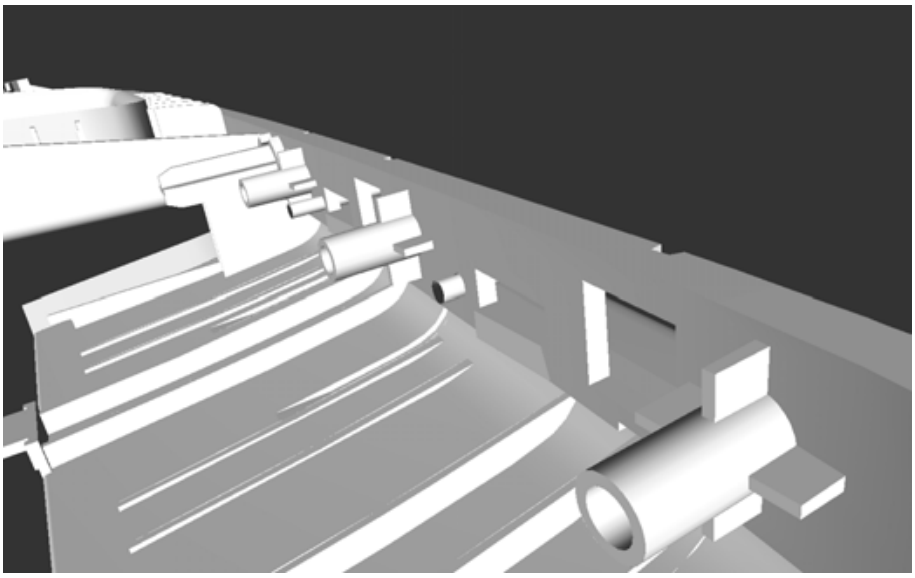

Figure 5.5: An example of a model with complex features, like ribs and bosses.

Identify the inconsistent elements

With the above concept of propagation, it is of utmost importance to accurately identify inconsistent elements. A proper identification of these elements will allow to significantly reduce the RMSE, as the thickness of correct elements will improve the thickness of the incorrect ones. On the other hand, if inconsistent elements are not correctly detected, then the concept of propagation fails, as it would propagate inaccurate thicknesses. Due to this, the combined approach, suggested in chapter 4, was modified to perform an error detection criteria that is capable of identifying inconsistent elements. Figure 5.6 shows the UML diagram that illustrates the behavior and data flow of the modified combined approach.

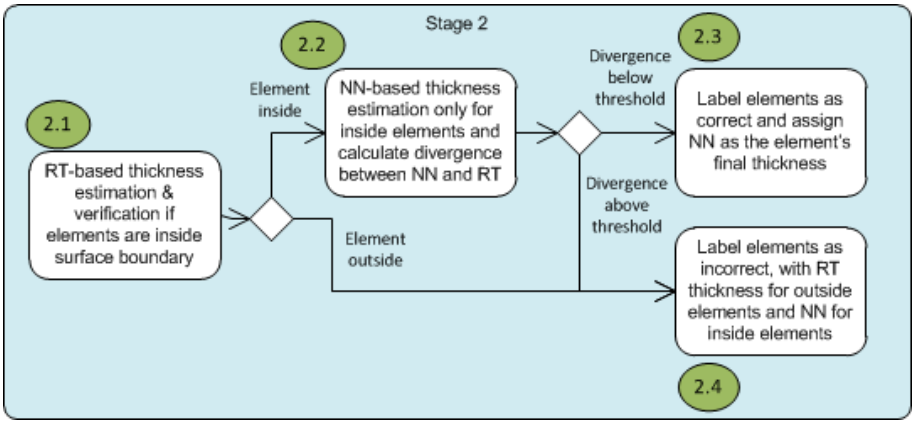

Figure 5.6: UML activity diagram. The diagram illustrates the behavior and overall data flow of the combined approach.

The first activity (2.1) of the combined approach uses ray tracing for

thickness estimation and to detect whether the mid-plane element is inside the boundaries of the surface. If the mid-plane element is inside, then nearest neighbor estimates a second thickness (2.2). With these two estimates, the following error detection criterion that aims to identify when such incorrect elements occur is defined:

- To identify the inconsistent elements that are inside the boundaries of the surface, an "error percentage" is given by the following equation: $\triangle_i = \frac{\left|T_i^{RT} - T_i^{NN}\right|}{max\left(T_i^{RT}, T_i^{NN}\right)}$, where T_i^{RT} and T_i^{NN} represent the local thickness estimates with ray tracing (RT) and nearest neighbor (NN), respectively, and $\Delta_i \in [0, 1]$ represents the "error percentage".
  By defining a threshold $\varepsilon \in [0, 1]$ to the maximum "error percentage" one is specifying the error detection criteria: elements with $\Delta > \varepsilon$ are considered inconsistent and tagged as incorrect. Otherwise they are tagged as correct. A maximum "error percentage" of 20° proved to be ideal (see section 5.2).

So, if the error detection criteria considers the element as correct, the nearest neighbor thickness estimate is assigned as the final thickness of the element (2.3). The choice of which estimate to use is irrelevant, since the difference between estimates is minimal. On the other hand, if the mid-plane element is considered incorrect, or if ray tracing detects it as being outside the boundaries of the surface (2.1), then the mid-plane element is tagged as incorrect (2.4). In such cases, a temporary thickness is assigned to the mid-plane element based on the element being detected as outside, where the thickness estimated by ray tracing (computing the differences between the two closest intersections from the same side) is used, or being detected as inside, in case the nearest neighbor estimate is used. Such information is then used for post-processing by the MFTAI.

Improving thickness accuracy

MFTAI's behavior is illustrated by the UML diagram shown in figure 5.7. The first activity of MFTAI (3.1) verifies whether any mid-plane element tagged as correct has a thickness that is above the maximum or below the minimum thicknesses specified by the user. This verification is essential to avoid that the thicknesses of false positives of correct mid-plane elements, identified during the error detection criteria, are used by the MFTAI for propagation. Those where this is true, are tagged as incorrect. A similar verification is performed in activity 3.3, but for elements whose thickness is below the minimum thickness specified by the user. As the minimum thickness is an optional parameter, the user may not specify it, in which case, the final thickness of the mid-plane element will be the nominal thickness, otherwise it will be the

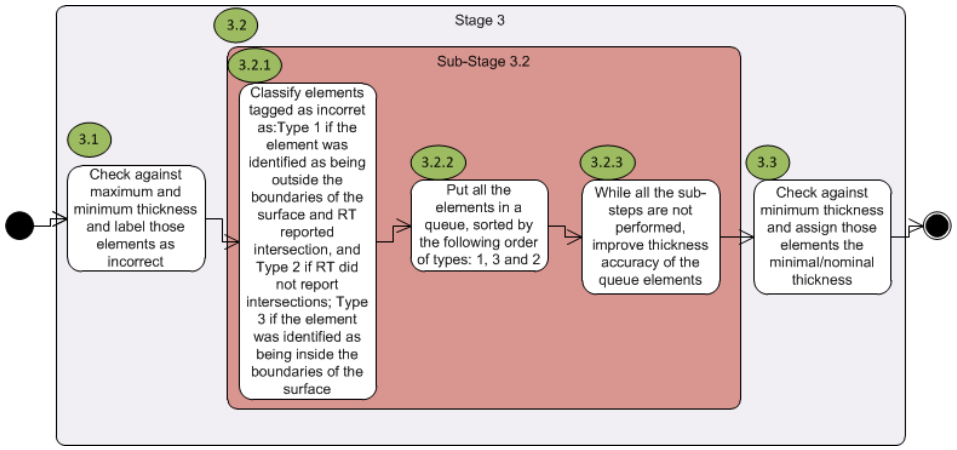

Figure 5.7: UML activity diagram. The diagram illustrates the behavior and overall data flow of the method for thickness accuracy approach.

specified minimum thickness. Activity 3.2.1 classifies the elements tagged as incorrect according to the information given by the ray tracing and nearest neighbor approaches: the mid-plane element is classified as type 1 if it was identified as being outside the boundaries of the surface and ray tracing reported intersections; type 2 if the mid-plane element was identified as being outside the boundaries of the surface but ray tracing did not report intersections; type 3 if the mid-plane element was identified as being inside the boundaries of the surface. This classification is important because it allows to define (in very roughly way) a partial order over the elements. Another ordering is performed that is omitted on the diagram of figure 5.7. For mid-plane elements that are classified as type 1, it is possible that their normals obliquely intersect the elements of the surface. Figure 5.8 illustrates how mid-plane elements in these situations can estimate inaccurate thicknesses: the rays shoot by mid-plane element A intersect the surface obliquely, which results in an overestimate thickness. It is then necessary to postpone the processing of these mid-plane elements, so that an accurate thickness can be assign by MFTAI. This is achieved by sorting type 1 mid-plane elements by the angle formed between their normals and the normal of the first element of the surface that they intersect, in descending order.

Activity 3.2.2 prepares the elements tagged as incorrect for activity 3.2.3. It creates a queue and sorts the elements by the following order: type 1, type 3 and type 2. This order insures that the elements with more likelihood of being accurately corrected by MFTAI are processed first: elements of type 2 should be processed after the elements of type 1 and type 3, because elements of type 2 do not intersect any element of the surface, and so, depend completely on the thickness of their neighbors; processing elements of type 3 after elements of type 1 resulted in a low RMSE when measuring how MFTAI improves the accuracy of the final thickness results (see section 5.3). Activity 3.2.3 is illustrated in the diagram (figure 5.7) as a "black box" due to its complexity.

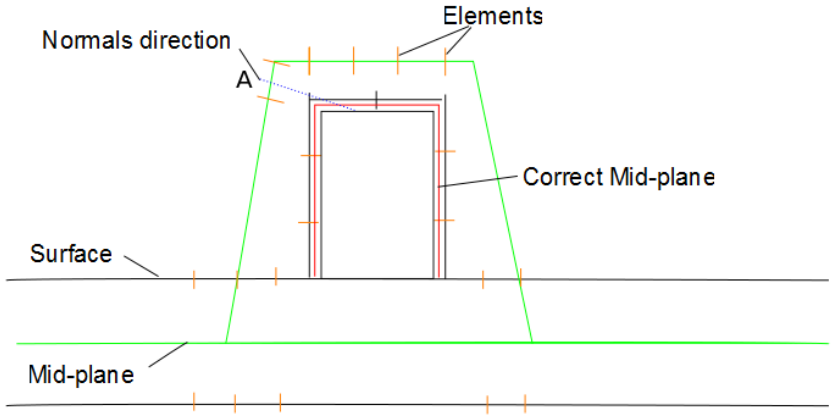

Figure 5.8: Illustration of how outside elements can intersect the elements of the surface. Element A incorrectly intersects the elements of the surface, resulting in inaccurate thickness estimation.

This activity is detailed in figure 5.9, where a diagram illustrates how the accuracy improvement is performed.

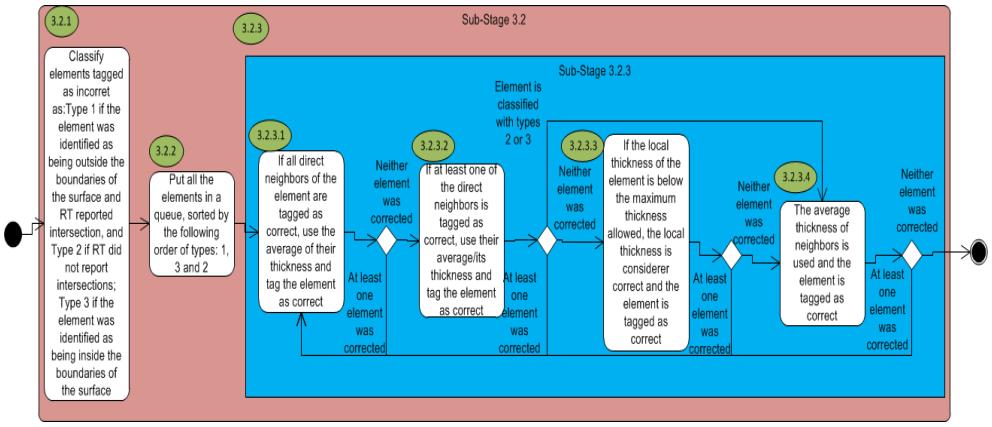

Figure 5.9: UML activity diagram. The diagram illustrates how the thickness accuracy of the incorrect elements is processed in the method for thickness accuracy improvement.

The basic behavior of the thickness accuracy improvement procedure (activity 3.2.3) is to subject all the elements in the queue to a series of activities that try to assign the best possible estimate of thickness to an element. For each activity (except 3.2.3.3), the incorrect elements are processed in the following order: type1, type3 and type 2. If during one of the activities, at least one element is corrected, the process restarts at activity 3.2.3.1. When activity 3.2.3.4 is reached and no corrections occur, the process reaches its end.

Activity 3.2.3.1 verifies which elements of the queue have all of their direct neighbors tagged as correct. For those where this is true the average thickness

of their direct neighbors is used. The elements that cannot be tagged as correct by activity 3.2.3.1 are subjected to activity 3.2.3.2, which verifies which elements have at least one of their direct neighbors tagged as correct. For those where this is true the average thickness of their correct direct neighbors is used. Activity 3.2.3.3 and 3.2.3.4 try to assign the best estimate of thickness for elements that have neither of their direct neighbors tagged as correct. Activity 3.2.3.3 is only executed for elements that are outside the boundaries of the surface. It verifies if their thickness is below the maximum and above the minimum thicknesses allowed, using the local thickness if such verification yields true. Activity 3.2.3.4 ignores the concept of direct neighbors and assigns the average thickness of the correct neighbors.

Required user input

MFTAI requires one mandatory and two optional parameters for its execution that must be specified by the user: the mandatory parameter is the maximum thickness of the part and the two optionals are the minimum thickness and the nominal thickness. The maximum thickness is used by MFTAI to verify if the local thickness of an element is a correct estimate (activity 3.1 and 3.2.3.3 in figures 5.7 and 5.9, respectively) and the minimum and nominal thicknesses are used to assign a value of thickness to elements that could not be corrected (activity 3.3 in figure 5.7). If the user does not specify these last two parameters, a minimum thickness of 0.2mm is assumed as default and an estimation of the nominal thickness is performed.

5.2 Sensitivity analysis on the angle limitation of neighbors and on the error detection criterion

The MFTAI presented in section 5 relies on the concepts of propagation and neighborhood in order to detect and improve the accuracy of inconsistent elements. These two concepts were materialized by the error detection criteria and by imposing a limit in the angle formed by the normals of two elements that are directly connected in Euclidean space. However, real world models' surfaces can be formed by different and complex features, like ribs, bosses, fillets, that, depending on the granularity and level of detail of the mid-plane mesh, can be approximated accurately, coarsely or even ignored at all. This can lead to poor mid-plane mesh representations, with elements that incorrectly approximate the surface. Also, and since the thickness of the different features can vary significantly from the rest of the model, MFTAI should avoid the propagation of thickness among mid-plane elements that represent different features.

Since the geometric characteristics of a real world part surface and its mid-plane granularity can change significantly, a sensitivity analysis was performed to: measure the best values for the maximum "error percentage" of the error detection criteria (called epsilon) and for the angle formed by the normals of two direct neighbors (called alpha) that are appropriate for a representative number of models; and whether the final results are very sensitive to variations on these values.

5.2.1 Sensitivity analysis methodology

In order to perform the measurement it is necessary to specify a measurand (the quantity to be measured). Usually, in sensitivity analysis, the measurand is specified by a description of a quantity, e.g., certain physical states and conditions. However, such specification is not able to convey what values of epsilon or alpha get the most accurate results: a quantity does not have the notion of locality, and so, it is not possible to infer if the thickness attributed to individual elements is the best estimate (the closest value to the exact local thickness). It is then necessary to specify the measurand by a value that conveys locality.

Such value can be obtained by comparing the thickness estimates with the exact values. By measuring the difference between the estimated values and the exact ones, one can not only study the individual differences, also called residuals, but can aggregate them into a single metric of precision power. This can be achieved with the RMSE (see section 4.1 in chapter 3).

The determination of the so called "exact values" for thickness was performed manually, so they must be understood as an approximation to the exact thickness in a given spot. Also, as the definition of thickness is ambiguous, in some locations it becomes necessary to define what thickness is the most appropriate: The thickness of an element that coarsely approximates a geometric feature is the thickness that would be computed if the geometric feature were perfectly represented (figure 5.10); if extremities of the model are not represented, the correct thickness for the elements that approximate that area should be estimated as if the surface were flat (figure 5.11); if the mid-plane mesh contains elements that incorrectly represent a inexistent geometry on the surface (figure 5.12), then they are ignored since its correct thickness is unknown (they are only ignored for this study).

5.2.2 Models and values sampled from the distribution of the epsilon and alpha parameters

For this analysis, three models were chosen due to their geometric characteristics and to their mid-plane mesh granularity and detail: B-Pillar Trim (figure 5.13) model contains many ribs and bosses and its coarse mid-plane mesh

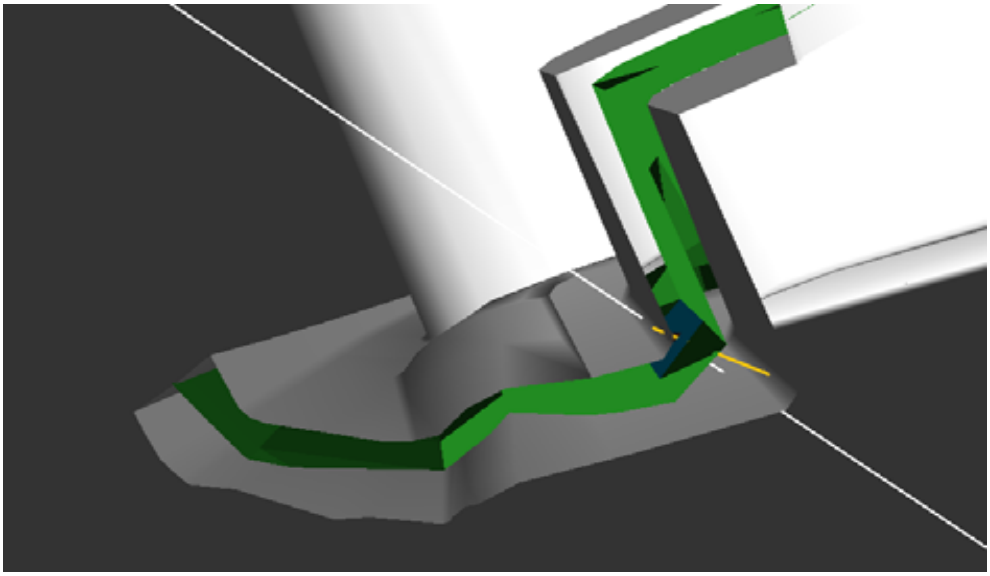

Figure 5.10: The surface of the Door Handle model (white) and the mid-plane mesh (green). The mid-plane element (blue) tries to approximate a fillet, but due to the coarse approximation, its normal (white line) intersects the incorrect surface elements. In this case the correct thickness should be the distance between the surface geometric primitives given by the orange line.

has approximately 56% of its elements outside the surface boundaries; Door Handle New (figure 5.14) model does not represent a closed surface (figure 5.15), which implies that the test of whether an element is inside or outside the boundary of the surface fails (the test is based on the point-in-polygon problem); Door Handle (figure 5.16) model is a simpler model which has a fine mid-plane mesh representation.

These three models were chosen because they illustrate the three possible cases that the CAD2FE tool has to handle: the Door Handle represents the case where the mid-plane mesh is fine and detailed; the B-Pillar Trim represents the case where the mid-plane mesh is coarse and poorly represents the surface and its geometric features; the Door Handle New represents a case were the surface is not closed and the mid-plane mesh is also coarse and poorly detailed. The sampling generation for the analysis consists in using a range of input values between 0% and 90% for the alpha parameter and 0% and 100% for the epsilon parameter, with increments of 5% for both (note that the value of 0% for epsilon is representative of an extreme case where none of the mid-plane elements is considered correct; obviously, such value should never be used). For the presentation of the analysis results, several figures were created that show the values of RMSE obtained with each parameter value for individual features (ribs and bosses) and for the complete three models.

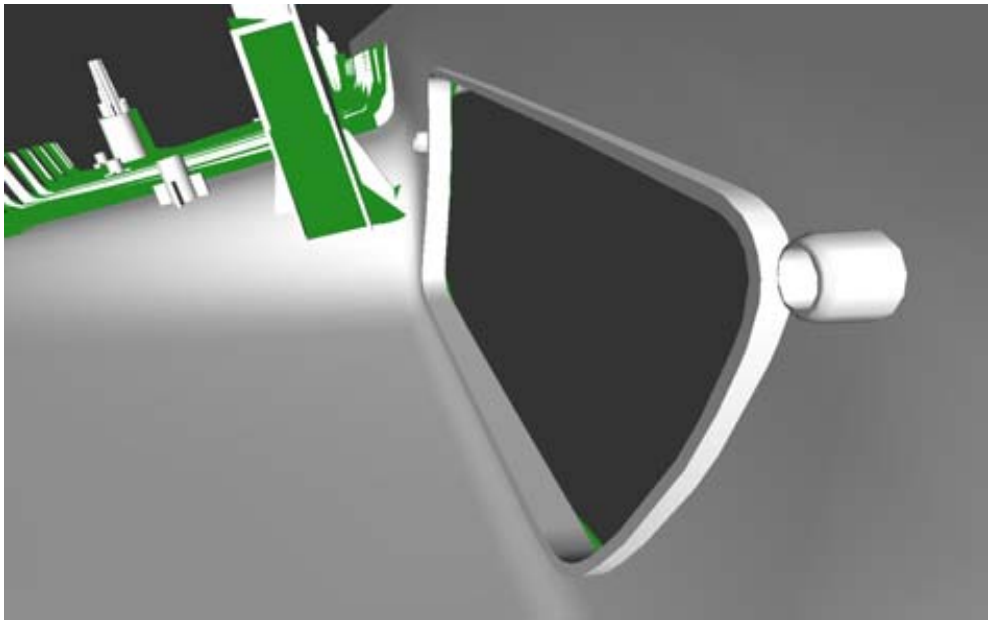

(a)

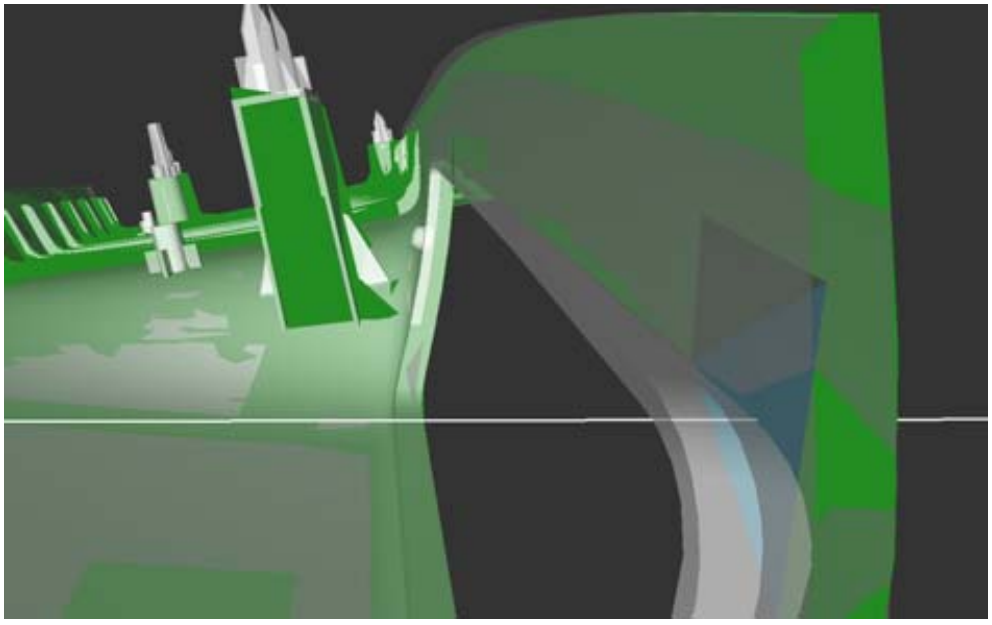

(b)

Figure 5.11: Figure 5.11(a) shows the surface (white) of the B-Pillar Trim where a feature raises in the extremities of the hole. In figure 5.11(b) it is visible that the mid-plane mesh (green) ignored this feature. The blue mid-plane element normal's (white line) intersects the raised feature, which will result in a overestimated thickness. The correct thickness for this element is considered to be the thickness estimated if the feature did not exist (i.e. the surface is considered flat).

5.2.3 Sensitivity analysis to epsilon parameter results

Two tests were performed in order to measure the best value of epsilon. The first test measures the direct impact of the epsilon parameter, i.e., only ele-

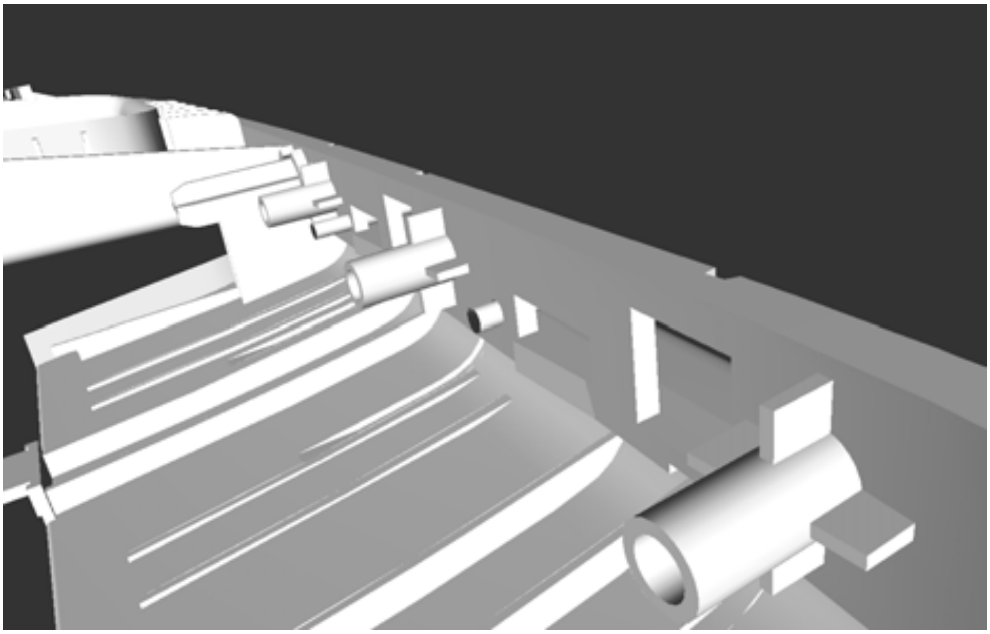

(a)

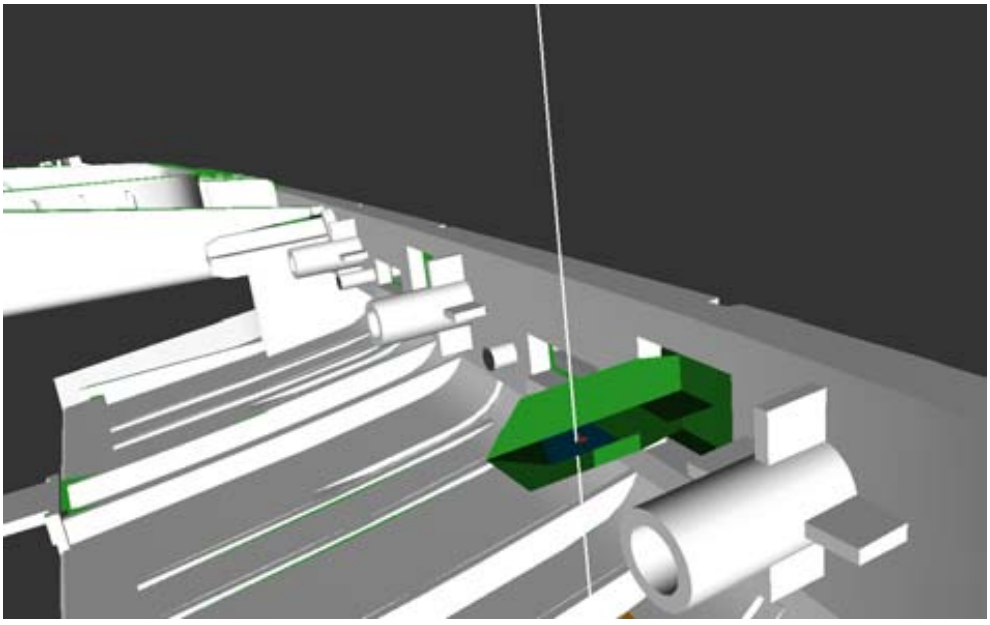

(b)

Figure 5.12: Figure 5.12(a) shows the surface (white) of the Door Handle New model. Figure 5.12(a) shows that the mid-plane mesh (green) has elements that approximate inexistent geometries. These mid-plane elements are ignored during the sensitivity analysis.

ments that are inside the boundaries of the surface contribute to the summation of RMSE. For this test only the B-Pillar Trim and Door Handle models were chosen, because in the Door Handle New MFTAI cannot correctly identify if a mid-plane element is inside or outside the boundaries of the surface.

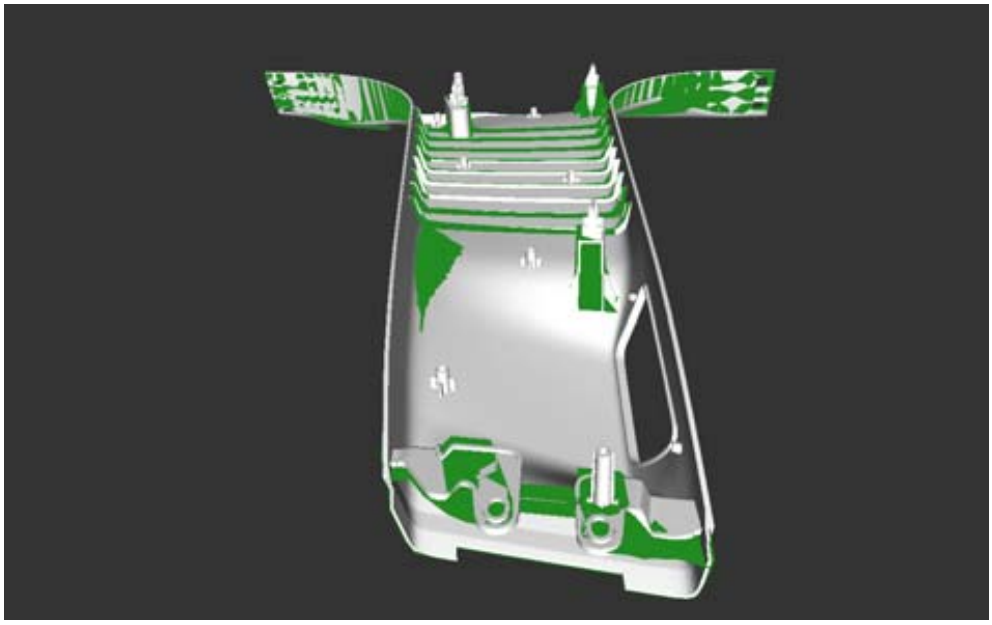

Figure 5.13: The surface (white) and mid-plane mesh (green) of the B-Pillar Trim model.

Figure 5.14: The surface (white) and mid-plane mesh (green) of the Door Handle New model.

Since the value of epsilon also has an indirect impact on the outside elements (due to the propagation), the second test considers all the inside and outside elements for all the three models. Figure 5.17 shows the RMSE values obtained for the first test and figure 5.18 shows the RMSE values obtained with the second test.

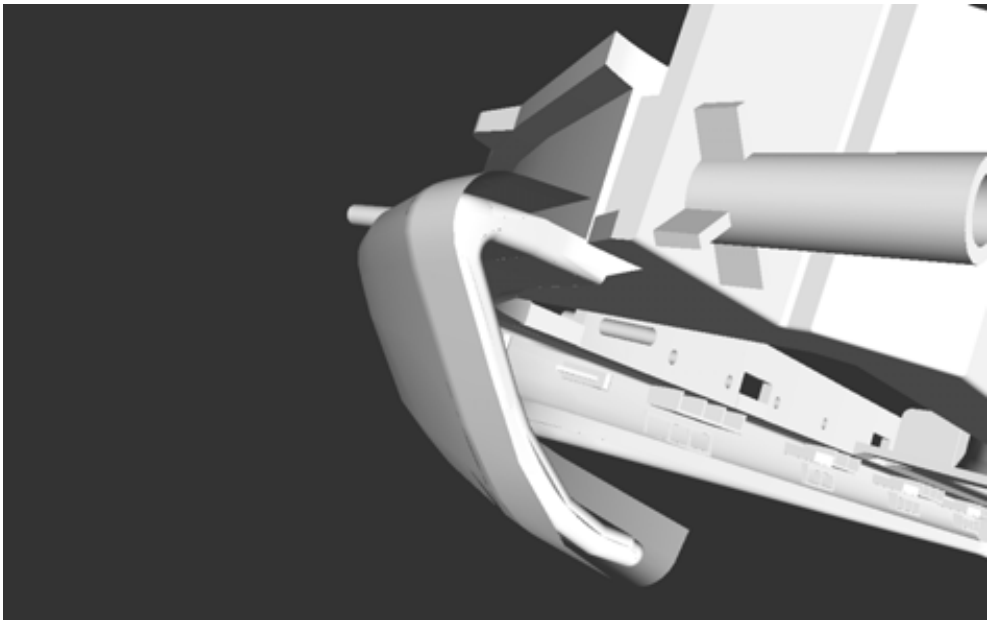

Figure 5.15: The outermost surface can be seen as cover sheet for the main surface of the model.

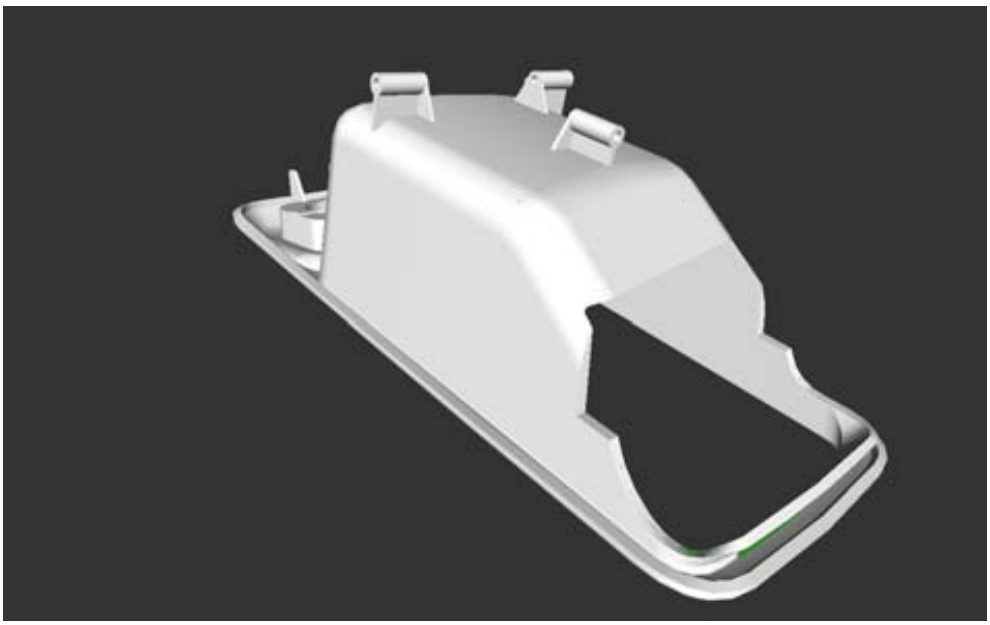

Figure 5.16: The surface (white) and the hardly visible mid-plane mesh (green) of the Door Handle model. The mid-plane mesh is very fine and is an accurate representation of the surface. Due to this the mid-plane mesh runs practically always inside the surface and thus is not visible.

5.2.4 Sensitivity analysis to alpha parameter results

Two types of tests were performed in order to measure the best value of alpha. The first type of tests measures the RMSE values obtained for individual

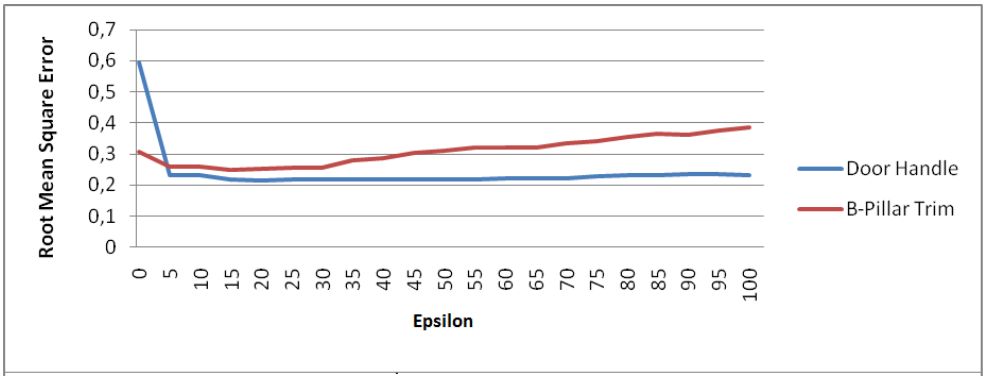

Figure 5.17: The RMSE values obtained with different input values for the epsilon parameter (the maximum "error percentage" between the thickness estimated by the RT and NN approaches) for the B-Pillar Trim models and Door Handle (figures 5.13 and 5.16) when only mid-plane elements that are inside the surface are considered.

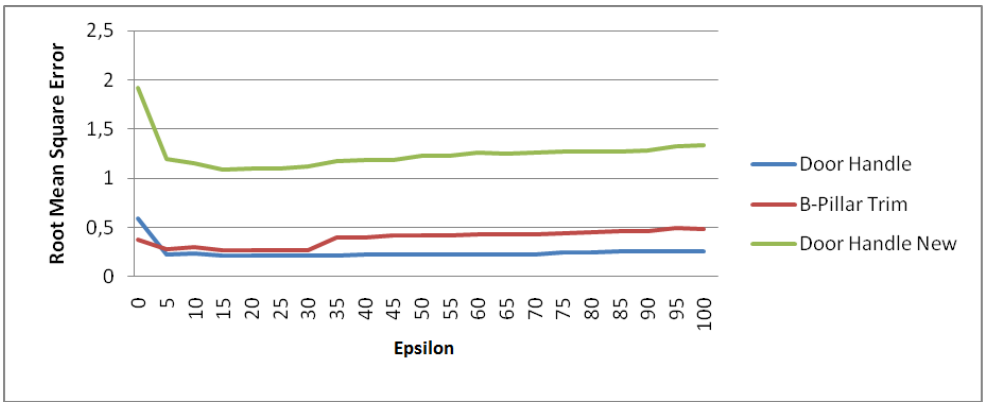

Figure 5.18: The RMSE values obtained with different input values for the epsilon parameter (the maximum "error percentage" between the thickness estimated by the RT and NN approaches) for the three models (figures 5.13 5.14 and 5.16) when all the mid-plane elements are considered.

geometric features. For this test only the B-Pillar Trim and the Door Handle New models were used, since the Door Handle model's mid-plane gives a good representation of the different features on the surface. Figure 5.19 identifies the geometries that were selected from the B-Pillar Trim model and figure 5.20 identifies the geometries selected from the DoorHandle New model.

Figure 5.21 and figure 5.22 show the RMSE values obtained for various features selected from the B-Pillar Trim model and the Door Handle New, respectively.

The second type of test measures the RMSE values obtained for all the mid-plane elements of the three models. Figure 5.23 shows the results obtained.

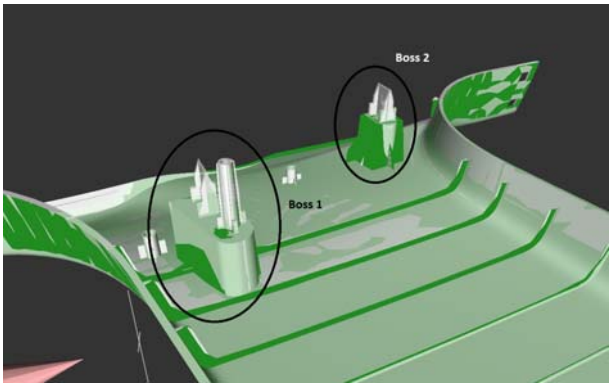

(a)

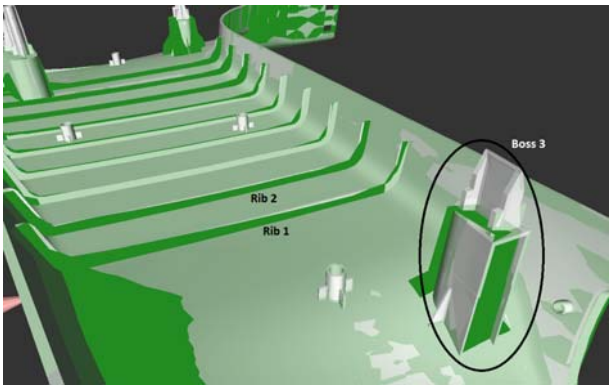

(b)

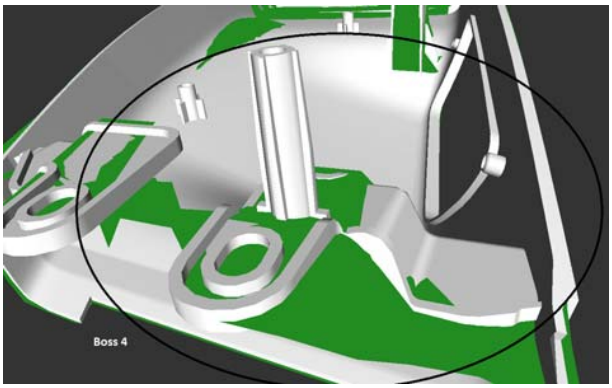

(c)

Figure 5.19: The various geometric features of the B-Pillar Trim model that were selected for the sensitivity analysis. The names in each image identify uniquely each of the features.

5.2.5 Results analysis

Epsilon parameter

Analyzing the RMSE results in figure 5.17, one can see that for the Door Handle model, the sensitivity to the value of the epsilon parameter is very small. Such results were expected because the mid-plane mesh appears to be

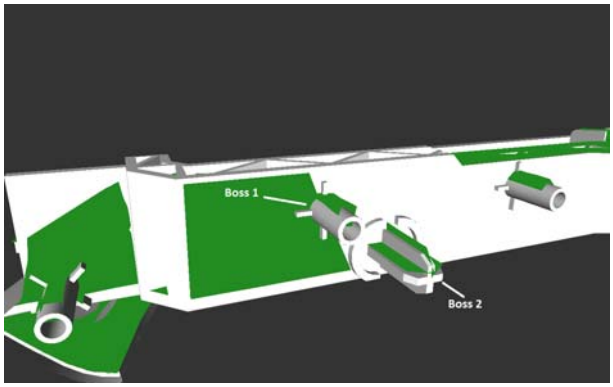

(a)

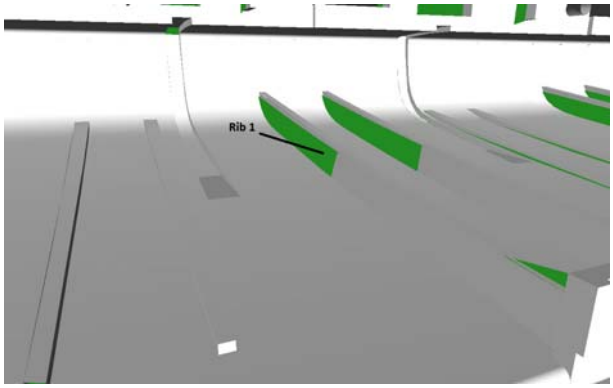

(b)

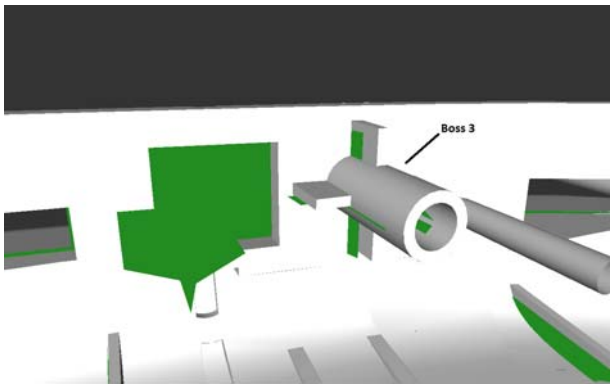

(c)

Figure 5.20: The various geometric features of the Door Handle New model that were selected for the sensitivity analysis. The names in each image identify uniquely each of the features.

accurate, as 99.5% of its elements are inside the surface boundary. Due to this, the expected divergences between the ray tracing and nearest neighbor approaches are very small (figure 5.24 shows the individual divergences between the ray tracing and nearest neighbor). For the B-Pillar Trim model the RMSE results show that for input values between 15% and 20%, the lowest value its reached. For input values above 20% the RMSE becomes gradually

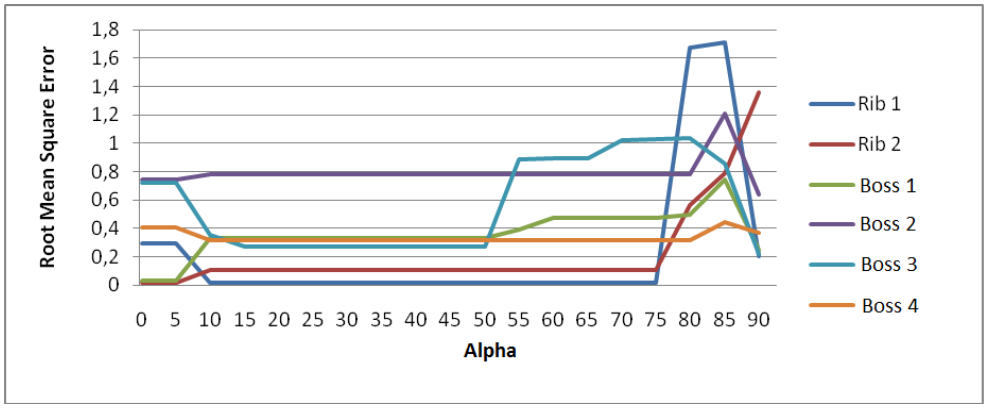

Figure 5.21: The RMSE values obtained with different input values for the alpha parameter (the maximum angle allowed between two direct neighbors) for the selected geometric features of the B-Pillar Trim model (figure 5.19).

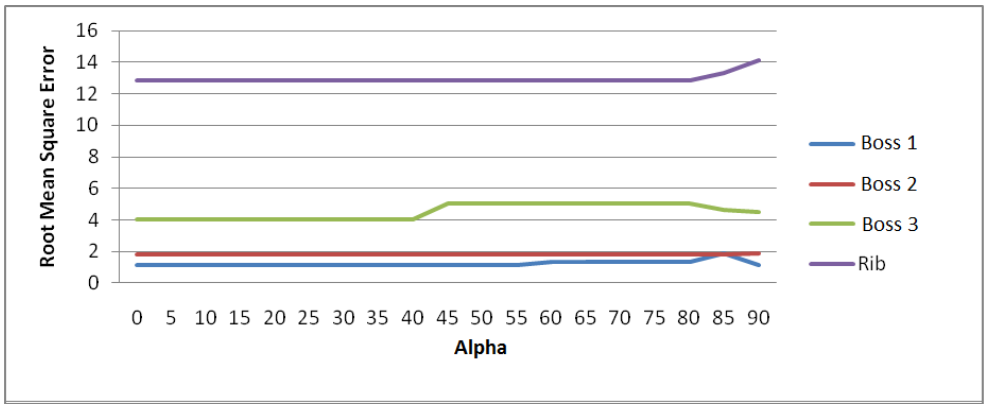

Figure 5.22: The RMSE values obtained with different input values for the alpha parameter (the maximum angle allowed between two direct neighbors) for the selected geometric features of the Door Handle New model (figure 5.20).

higher.

Figure 5.18 shows that for both Door Handle and B-Pillar Trim, the RMSE results obtained for the various values of the epsilon parameter mirrors the ones presented in figure 5.17. As the Door Handle model have 99.5% of its mid-plane elements inside, the results shown in figure 5.17 and 5.18 are virtually the same. For the B-Pillar Trim, the lowest value of RMSE is reached in the same interval of input values of the figure 5.17: 15% to 20%. Also, for input values above 20%, the same behavior is observed, the RMSE becomes gradually higher. For the Door Handle New, the same results of the other two models can be observed: the lowest RMSE value is reached at the interval between 15% to 20% and above 20% the RMSE becomes gradually higher.

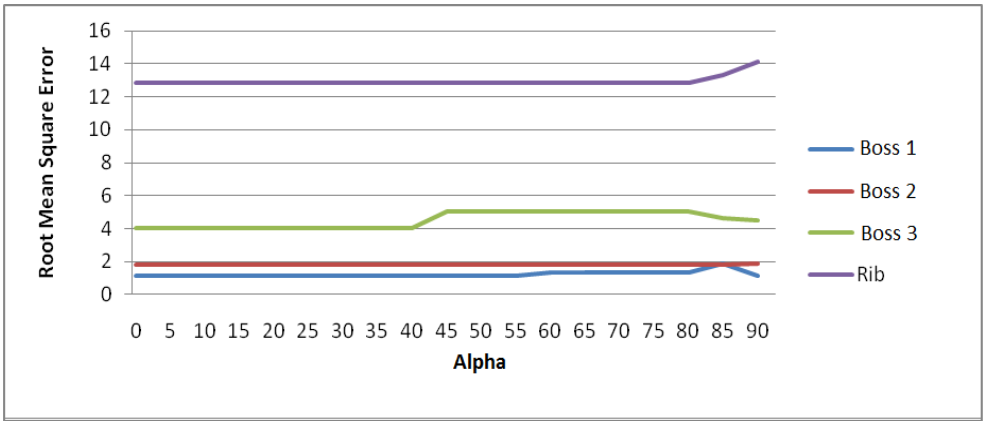

Figure 5.23: The RMSE values obtained with different input values for the alpha parameter (the maximum angle allowed between two direct neighbors) for the three models (figures 5.13, 5.14 and 5.16).

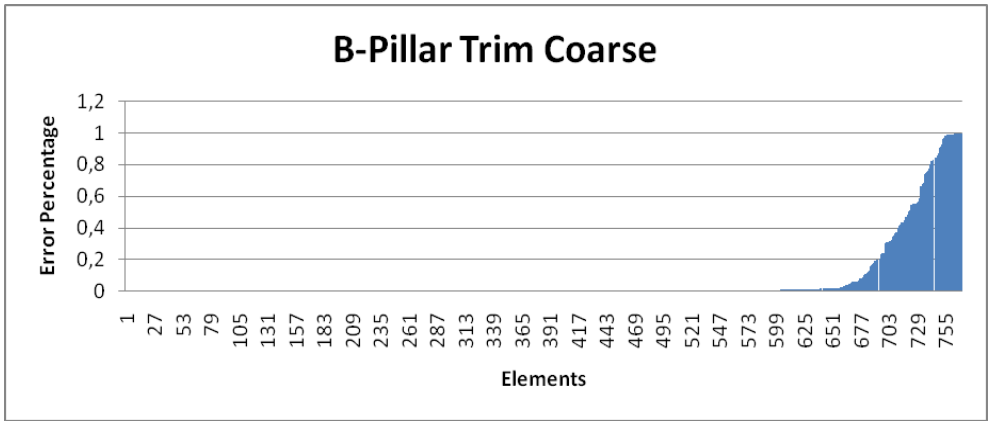

Figure 5.24: The individual error percentage (divergence between the ray tracing and nearest neighbor thickness) of the mid- plane elements that are inside the boundaries of the B-Pillar Trim surface. For approximately 85% of the elements, the divergence is in the interval]0%,1%].

Alpha parameter

Figure 5.21 presents interesting and, at first, contradictory results. While the RMSE for rib 1, boss 3 and boss 4 reach its minimum for 10°, 15° and 10°, respectively, the RMSE of rib 2, boss 1 and boss 2 reaches its minimum at 5°, and becomes gradually higher for values above 5°. This contradiction exposes one limitation of MFTAI: by assigning low values to alpha, such as 5°, the search for direct neighbors is narrowed. This implies that the MFTAI uses the local thickness more often for correctness, instead of using the thickness of, otherwise, direct neighbors. As described in sub-section 5.1 of "Thickness accuracy improvement method", when a mid-plane element is tagged as incorrect, the MFTAI searches for direct neighbors that are tagged as correct. If it can not find at least one, it verifies if the local thickness of

the element is below the maximum thickness allowed. If this is true, the local thickness of the element is consider the correct one.

Although this limitation can lead to better results for individual geometric features, Figure 5.23 shows that this is not true when considering all the surface of the model. In both DoorTrim New and B-Pillar Trim models, the lowest value of RMSE is reached at 20°. For the Door Handle model, due to its fine and accurate mid-plane mesh, the RMSE remains virtually the same for input values between 0° and 85°. Only when allowing a maximum angle of 90° is the RMSE affected (All the geometric features of the Door Handle model form an, almost, 90° angle between the surface, as shown in figure 5.25. With a 90° value of alpha, the mid-plane elements of the surface and the geometric features are allowed to "propagate" their thickness, which results in assigning wrong thickness for several elements). Thus, the common range for which lowest RMSE values are obtained is between 20°e and 60°.

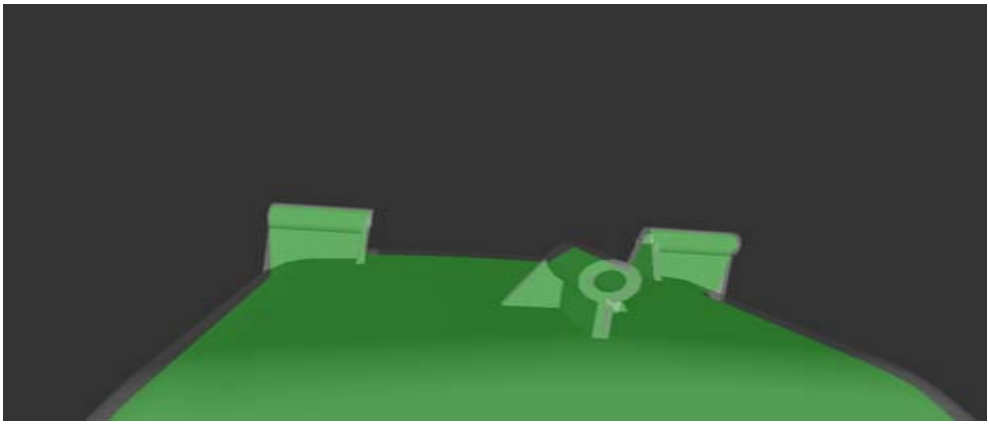

Figure 5.25: Some of the geometric features that form the Door Handle model. As can be seen, the angle formed between the surface (bottom green zone) and these geometric features is, approximately, 90°.

5.3 MFTAI Results

In order to measure how the MFTAI improves the accuracy of the final thickness results, the methodology used in section 5.2 ("Sensitivity analysis on the angle limitation of neighbors and on the error detection criterion") was used. Basically, the exact thickness of three models was determined manually. For each model, the individual differences between the exact values and the ones estimated by the CAD2FE tool are compared. The RMSE is used in order to aggregate these individual differences into a single measure of predictive power. The three models chosen (represented in figures 5.13, 5.14 and 5.16), illustrate the three possible cases that the CAD2FE tool has to handle: the Door Handle represents the case where the mid- plane mesh is fine and detailed; the B-Pillar Trim represents the case where the mid-plane mesh is

coarse and poorly represents the surface and its geometric features; the Door Handle New represents a case were the surface is not closed and the mid-plane mesh is also coarse and poorly detailed.

Table 5.1 shows the RMSE values obtained for each model with and without MFTAI.

	No MFTAI	MFTAI
Door Handle	0.232102	0.219882
B-Pillar Trim	3.847084	0.270773
Door Handle New	15.477623	1.086898

Table 5.1: RMSE results obtained for each model with the different types of accuracy improvements

5.4 Conclusions

With the modifications introduced by the MFTAI, the problems presented in chapter 4 are successfully avoided: by using a combined approach, the estimates of thickness of the ray tracing and nearest neighbor approaches allow the method to safely assess if the combined approach fails to estimate an accurate thickness; ray tracing can be used to estimate the local thickness of an outside element that has no correct direct neighbors, comparing it with the maximum thickness allowed, to safely assess if the local thickness is a good estimate; MFTAI also allows to assign a good estimate of thickness to mid-plane elements that, otherwise, would have an overestimate or a 0mm thickness. By propagating the thickness among correct mid-plane elements, it is highly probable that a very accurate thickness can be assigned.

The sensitivity analysis performed on the epsilon and alpha parameters shows that when the model is accurately represented by a fine mesh, the final results are not sensitive to these parameters. However, for coarse and poor approximations, sensitivity analysis shows that the lowest RMSE values for the epsilon and alpha parameters are obtained with values between 15% and 20% and between 20ºand 30º, respectively. In order to assign the best values for epsilon and alpha that are appropriate for a representative number of models, and since models that accurately represented are not sensitive to these parameters, epsilon is set to 20% and alpha to 25º.

Chapter 6

Conclusions

This thesis has presented a methodology to map the local thicknesses of computer-aided design (CAD) models to two dimensional crash simulation meshes (mid-plane). The common approach to determine mid-plane meshes thickness is to assign an averaged, usually the nominal, thickness to all the mid-plane elements. This is a very rough approximation and induces unnecessary error in the calculations.

Two approaches based on computer graphic's ray tracing and nearest neighbor 3D range search were developed that are able to estimate thicknesses from CAD models and map them into their mid-plane meshes representations. These approaches were tested with virtual test specimens and found to estimate inaccurate thicknesses when certain geometric configurations occur. Also, the limitations on the generation of mid-plane mesh representations of the CAD models, which are based on highly time consuming manual work, results in meshes with limited accuracy, preventing the approaches to estimate accurate thicknesses. A thorough study of the approaches behavior was performed in order to quantitatively assess their accuracy, allowing, not only to identify the situations that lead to inaccurate thickness estimations, but also to suggest a combination of the approaches. This lead to the development of a method for thickness accuracy improvement (MFTAI) that is able to identify, based on the information retrieved by both approaches, when the mid-plane element is likely to be assigned an inaccurate thickness: using ray tracing to detect whether an element's centroid is outside the boundaries of the surface; and computing the differences between the thicknesses estimated by both approaches, checking if their difference is above a defined threshold, which indicates that the thickness estimated by one or both approaches may be inaccurate. These elements are then processed by MFTAI and subjected to a thicknesses propagation scheme, which improves their thickness accuracy based on the thickness of correct neighbors.

The final outcome of this thesis is a software package, named CAD2FE, that is able to map the local thicknesses of CAD models to their mid-plane meshes representations. CAD2FE uses a novel approach to estimate thick-

nesses of CAD models and assess their accuracy, using a method to improve the accuracy of the thickness of elements identified as inconsistents. The integration of the thickness estimation approach and the method of thickness accuracy improvement allows to use not only fine mid-plane mesh representations of CAD models, but also the more common and computationally less expensive coarse mid-plane mesh representations, guaranteeing that thicknesses of 0mm or thicknesses above the maximum thickness of the CAD model do not occur. This allows engineers to benefit from an accurate and precise way of mapping the thickness distribution of CAD models to mid-plane meshes, empowering accurate car crash simulations.

Chapter 7

Future Work

This thesis has presented a methodology to the thickness estimation of computer-aided design (CAD) models. A quantitative and systematic analysis as well as methodology study of the thickness estimation accuracy has been used on a number of test cases. The results obtained with several CAD models of real world parts and different mid-plane meshes granularities has proven that the proposed methodology can be used to estimate accurate thicknesses even when the mid-plane mesh has inaccuracies. However, the current supported CAD models are limited to the ones that use discrete representations. Further work would need to be undertaken to embrace CAD models with Non-uniform rational B-spline geometry and/or boundary representation. Also, the current methods available to generate mid-plane meshes are limited, inaccurate, and prevent fully exploring the advantages of modeling and simulation tools. Further development of the tool to support the generation of accurate mid-plane surfaces of CAD geometries could avoid the inaccuracies that may still persist in the current thickness estimation methodology.

Bibliography

[AL02] A. Atramentov and S.M. LaValle. Efficient nearest neighbor searching for motion planning. In *Proceedings- IEEE International Conference on Robotics and Automation*, volume 1, pages 632–637. Citeseer, 2002.

[AMN+98] Sunil Arya, David M. Mount, Nathan S. Netanyahu, Ruth Silverman, and Angela Y. Wu. An optimal algorithm for approximate nearest neighbor searching fixed dimensions. *J. ACM*, 45(6):891–923, 1998.

[App68] A. Appel. Some techniques for machine rendering of solids. In *AFIPS Conferences*, volume 32, pages 37–45, 1968.

[Arm94] C.G. Armstrong. Modelling requirements for finite-element analysis. *Computer-Aided Design*, 26(7):573–578, 1994.

[ATP84] D.A. Anderson, J.C. Tannehill, and R.H. Pletcher. *Computational fluid mechanics and heat transfer*. Hemisphere New York, 1984.

[BA08] AL Braun and AM Awruch. Finite element simulation of the wind action over bridge sectional models: Application to the Guamá River Bridge (Pará State, Brazil). *Finite Elements in Analysis & Design*, 44(3):105–122, 2008.

[BBKK97] S. Berchtold, C. Böhm, D.A. Keim, and H.P. Kriegel. A cost model for nearest neighbor search in high-dimensional data space. In *Proceedings of the sixteenth ACM SIGACT-SIGMOD-SIGART symposium on Principles of database systems*, pages 78–86. ACM, 1997.

[BKK96] Stefan Berchtold, Daniel A. Keim, and Hans P. Kriegel. The x-tree: An index structure for high-dimensional data. In T. M. Vijayaraman, Alejandro P. Buchmann, C. Mohan, and Nandlal L. Sarda, editors, *Proceedings of the 22nd International Conference on Very Large Databases*, pages 28–39, San Francisco, U.S.A., 1996. Morgan Kaufmann Publishers.

[BNPvE08] M. Brinkmeier, U. Nackenhorst, S. Petersen, and O. von Estorff. A numerical model for the simulation of tire rolling noise. *Journal of Sound and Vibration*, 309(1):20–39, 2008.

[BT71] KG Budden and PD Terry. Radio ray tracing in complex space. *Proceedings of the Royal Society of London. Series A, Mathematical and Physical Sciences*, 321(1546):275–301, 1971.

[CH67] T. Cover and P. Hart. Nearest neighbor pattern classification. *IEEE Transactions on Information Theory*, 13(1):21–27, 1967.

[Cha74] C.L. Chang. Finding prototypes for nearest neighbor classifiers. *IEEE Transactions on Computers*, 100(23):1179–1184, 1974.

[dB08] Mark de Berg. *Computational Geometry: Algorithms and Applications*. Springer, 3rd edition, 2008.

[DeG80] Morris H. DeGroot. *Probability and Statistics*. Addison-Wesley, 2nd edition, 1980.

[DWS04] A. Dietrich, I. Wald, and P. Slusallek. Interactive visualization of exceptionally complex industrial CAD datasets. In *ACM SIGGRAPH 2004 Sketches*, page 27. ACM, 2004.

[Ebe] D. Eberly. Distance between point and triangle in 3d. *Magic Software, http://www. magic-software. com/Documentation/pt3tri3. pdf*.

[Ede01] Herbert Edelsbrunner. *Geometry and Topology for Mesh Generation*. Cambridge University Press, 2001.

[FG00] Pascal Jean Frey and Paul-Louis George. *Mesh Generation: Application to Finite Elements*. Hermes Science, 2000.

[FTAE02] H. Ferhatosmanoglu, E. Tuncel, D. Agrawal, and A. El Abbadi. Approximate nearest neighbor searching in multimedia databases. In *Data Engineering, 2001. Proceedings. 17th International Conference on*, pages 503–511. IEEE, 2002.

[GBGP02] D. Gesbert, H. Bolcskei, D. Gore, and A. Paulraj. MIMO wireless channels: Capacity and performance prediction. In *Global Telecommunications Conference, 2000. GLOBECOM'00. IEEE*, volume 2, pages 1083–1088. IEEE, 2002.

[GG91] Allen Gersho and Robert M. Gray. *Vector quantization and signal compression*. Kluwer Academic Publishers, Norwell, MA, USA, 1991.

[HC] D. Henrich and X. Cheng. Fast distance computation for on-line collision detection with multi-arm robots. In *IEEE International Conference on Robotics and Automation, Nice, France, May*, volume 10, pages 2514–2519. Citeseer.

[HDSB01] K.H. Huebner, D.L. Dewhirst, D.E. Smith, and T.G. Byrom. *The finite element method for engineers, 4th edition*. Wiley-Interscience, 2001.

[HO08] A. Hawkins and J. T. Oden. Toward a predictive model of tumor growth. Technical report, Institute for Computational Engineering and Sciences (ICES), The University of Texas at Austin, November 2008.

[HPR00] J.H. Han, M. Pratt, and W.C. Regli. Manufacturing feature recognition from solid models: a status report. *IEEE Transactions on Robotics and Automation*, 16(6):782–796, 2000.

[J.J95] J.J. Shah and M. Mantyla. *Parametric and feature-based CAD/CAM: concepts, techniques, and applications*. A Wiley-Interscience Publication, John-Wiley & Sons, Inc., 1995.

[KGW+99] S.C. Kim, B.J. Guarino Jr, T.M. Willis III, V. Erceg, S.J. Fortune, R.A. Valenzuela, L.W. Thomas, J. Ling, and J.D. Moore. Radio propagation measurements and prediction using three-dimensional ray tracing in urban environments at 908 MHz and 1.9 GHz. *IEEE Transactions on Vehicular Technology*, 48(3):931, 1999.

[KLP06] V.P. Kumar, R. Lakkumanan, and K. Prakasan. Computer aided optical design of reflectors in automotive headlights. *Proceedings of the Institution of Mechanical Engineers, Part D: Journal of Automobile Engineering*, 220(4):415–424, 2006.

[KPSC06] B. Kirk, J. W. Peterson, R. H. Stogner, and G. F. Carey. libmesh: A c++ library for parallel adaptive mesh refinement/coarsening simulations. *Engineering with Computers*, 22(3):237–254, 2006.

[KSF+96] F. Korn, N. Sidiropoulos, C. Faloutsos, E. Siegel, and Z. Protopapas. Fast nearest neighbor search in medical image databases. In *Proceedings of the International Conference on Very Large Data Bases*, pages 215–226. Citeseer, 1996.

[LG05] H.L. Lockett and M.D. Guenov. Graph-based feature recognition for injection moulding based on a mid-surface approach. *Computer-Aided Design*, 37(2):251–262, 2005.

[Löh08] Rainald Löhner. *Applied computational fluid dynamics techniques: an introduction based on finite element methods; 2nd edition*. Wiley, 2008.

[PCC09] V. Petrovic, P.R. Castellano, and R.T. Carot. Manufacturability analysis of injected parts based on a mid-surface approach. *Journal of Engineering Design*, 20(6):627–644, 2009.

[RHS08] N. Rawlinson, J. Hauser, and M. Sambridge. Seismic ray tracing and wavefront tracking in laterally heterogeneous media. volume 49 of *Advances in Geophysics*, pages 203–273. Elsevier, 2008.

[SF73] Gilbert Strang and George Fix. *An Analysis of The Finite Element Method*. Prentice Hall, 1973.

[SK08] K. Sathyanarayana and G.V.V. Kumar. Evolution of computer graphics and its impact on engineering product development. In *Computer Graphics, Imaging and Visualisation, 2008. CGIV '08. Fifth International Conference on*, pages 32–37, Aug. 2008.

[SPW08] E. De Sturler, G. H. Paulino, and S. Wang. Topology optimization with adaptive mesh refinement. In J. F. Abel and J. R. Cooke, editors, *Proceedings of the 6th Internation Conference on Computation of Shell and Spatial Structures IASS-IACM 2008: Spanning Nano to Mega 28-31 May 2008, Cornell University, Ithaca, NY, USA*, 2008.

[SR94] S.Y. Seidel and T.S. Rappaport. Site-specific propagation prediction for wireless in-building personal communication system design. *IEEE transactions on Vehicular Technology*, 43(4):879–891, 1994.

[TWM85] J. Thompson, Z. Warsi, and C. Mastin. *Numerical Grid Generation: Foundations and Applications*. North Holland, Elsevier, 1985.

[Č01] Vlastislav Červený. *Seismic ray theory*. Cambridge University Press, Cambridge, UK, 2001.

[VHK+90] Mark Vandewettering, Eric Haines, Edward John Kalenda, Richard Parent, Sam Uselton, "Za" Andersson, and Bruce Holloway. Point in Polygon, One More Time...,. In Eric Haines, editor, *Ray Tracing News*, volume 3. 1990.

[WBDS03] I. Wald, C. Benthin, A. Dietrich, and P. Slusallek. Interactive ray tracing on commodity pc clusters. *Euro-Par 2003 Parallel Processing*, pages 499–508, 2003.

[WG66] Jr. William Weaver and James M. Gere. *Matrix Analysis Of Framed Structures*. Springer-Verlag New York, 3rd edition, 1966.

[WH06] I. Wald and V. Havran. On building fast kd-trees for ray tracing, and on doing that in O (N log N). In *Proceedings of the 2006 IEEE Symposium on Interactive Ray Tracing*, volume 4. Citeseer, 2006.

[Whi80] Turner Whitted. An improved illumination model for shaded display. *Communications of the ACM*, 23(6):343–349, 1980.

[WLL+05] YY Wang, C. Lu, J. Li, XM Tan, and YC Tse. Simulation of drop/impact reliability for electronic devices. *Finite Elements in Analysis & Design*, 41(6):667–680, 2005.

[Wri06] Peter Wriggers. *Computational contact mechanics; 2nd edition.* Springer Verlag: Heidelberg, 2006.

[Yan86] T.Y. Yang. *Finite element structural analysis.* Prentice-Hall Englewood Cliffs, NJ, 1986.

[Yia93] Peter N. Yianilos. Data structures and algorithms for nearest neighbor search in general metric spaces. In *SODA '93: Proceedings of the fourth annual ACM-SIAM Symposium on Discrete algorithms*, pages 311–321, Philadelphia, PA, USA, 1993. Society for Industrial and Applied Mathematics.

[Yiu00] P. Yiu. The uses of homogeneous barycentric coordinates in plane euclidean geometry. *International Journal of Mathematical Education in Science and Technology*, 31(4):569–578, 2000.

[ZT00] O.C. Zienkiewicz and R.L. Taylor. *The finite element method. Fifth Edition. Volume 1: The Basis.* Butterworth-Heinemann, Oxford, 2000.